Carbon – Science and Technology
ISSN 0974 – 0546
http://www.applied-science-innovations.com

INVITED REVIEW ARTICLE Received : 24/12/2013, Accepted :30/12/2014

EXTENDING THE APPLICATIONS OF BODIPY TO THE WHOLE VISIBLE SPECTRAL REGION

Jorge Bañuelos* and Iñigo López Arbeloa

Departamento de Química Física, Universidad del País Vasco UPV/EHU, Apartado 644, 48080–Bilbao, Spain.

*Corresponding autor:
Dr. J. Bañuelos Prieto
Phone: +34 94 601 27 11
Fax: +34 94 601 35 00
E–mail: jorge.banuelos@ehu.es

Keywords: BODIPY, Photophysics, Quantum Mechanics, Substituent Effect, Laser dyes, Singlet Oxygen

Content:

1. Introduction:

The scientific community in multidisciplinary areas has intensively studied fluorescent dyes. Currently, the technological interest of these dyes has allowed their successful application in many different fields, for instance, as active media of tunable lasers, in the development of photoelectronic devices, as fluorescent probes and chemical sensors, or as tools for monitoring the physicochemical characteristics of the surrounding environment [1–7]. Knowledge of the photophysical properties of these systems is essential, not only for

understanding the process underlying their potential applications, but also for designing new dyes with tailor-made properties.

Among the large number of existing laser dye families covering the spectral region from UV to near–IR [1], 4,4–difluoro–4-bora–3a,4a–diaza–s–indacenes (herein named BODIPY) have received special attention in recent years [8–13]. Their basic structure, depicted in Scheme 1, consists of two pyrrole rings linked by a methine group and a BF_2 bridge. The first report of these fluorophores dates from 1968 by Treibs and Keuzer [14], but they did not gain recognition from the scientific community until the end of the 90s, when some reports by Boyer and Pavlopoulos showed their potential application in tunable dye lasers [15–18]. The promising results obtained encouraged other investigators to search for a deeper understanding of the lasing behavior and to use this dye family in other fields such as biology or medicine [19–23]. Indeed, a large number of publications were available in a short period of time, describing their properties and applications and becoming a booming area of research.

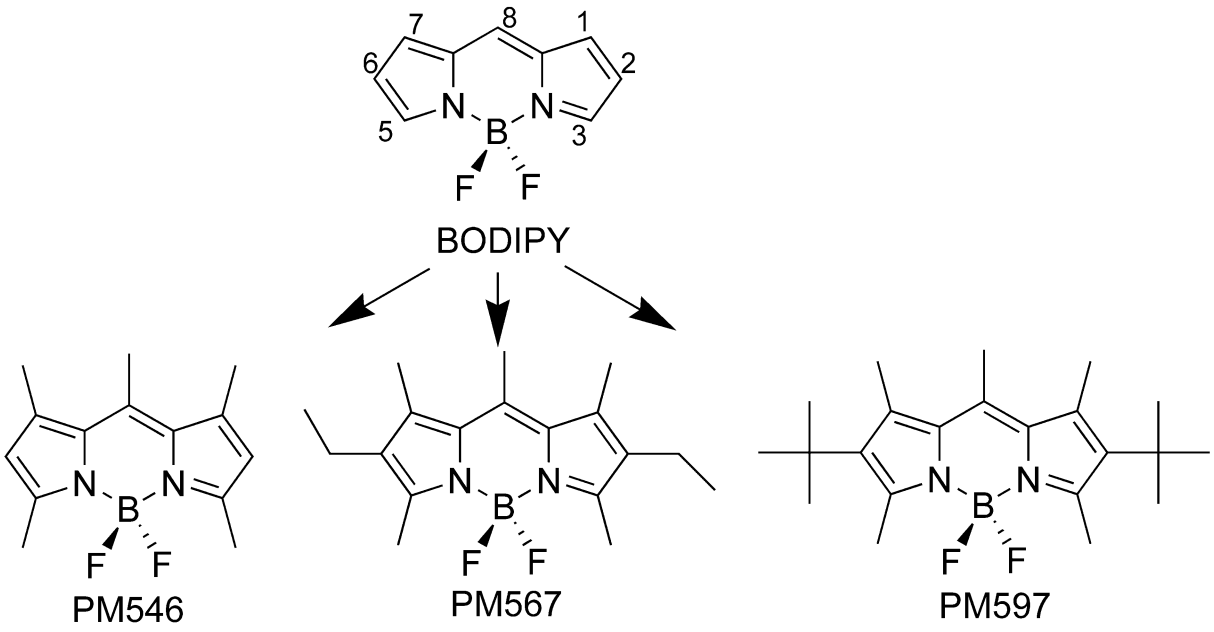

Scheme (1): Molecular structure of BODIPY and their alkylated commercial derivatives; PM546, PM567 and PM597.

BODIPY laser dyes are characterized by strong absorption and fluorescence bands in the middle area (green–yellow) of the visible spectral region, with notable high fluorescent [23–31] and lasing efficiencies [8,32–34]. Their versatility, chemical robustness, low triplet state population, and thermal and photochemical stability enhance the photoresponse of these dyes. For instance, even after several pumping pulses, BODIPY keeps their bright lasing signals, particularly when incorporated in solid host matrices [35–39]. The development of solid−state tunable dye lasers is of interest for commercial and technological applications because they have inherent advantages with respect to liquid–state lasers, including a better manageability, versatility, and miniaturization of the experimental setup, and are devoid of toxic and flammable solvents.

A large number of publications have claimed the use of BODIPY dyes in different photoelectronic devices, apart from the above commented laser application: for instance, as

light harvesting arrays and antenna systems [40–48], acting as energy injectors or acceptors to collect light and carry it to a specific reaction centre; or in holographic systems for digital information storage [49–51]. Moreover, many reports have described the use of BODIPY as fluorescent probes or chemical sensors in biomedicine and biochemistry. The photophysics of BODIPY have to be sensitive to environmental properties [52–56] or to the presence of an analyte in the surrounding medium [57–64]. Usually, these probes or sensors are achieved by the incorporation of specific functional groups in the BODIPY core, promoting new deactivation processes that are sensitive to environmental conditions (*i.e.*, photoinduced charge transfer). These processes quench the fluorescence of the dye, and the sensor behaves as a fluorescent on/off switch system depending on environmental conditions.

The understanding of the photophysical behavior of BODIPY dyes is essential for their use in technological applications such as lasing action, energy transport, or sensing process, and for designing new devices based on BODIPY. To this aim, quantum mechanical calculations have become a powerful tool to design new molecular structures with specific photophysical properties [65–69]. In general, most of these broad applications of BODIPY are based on the possibility to control and modulate the photophysical properties of the chromophore by the substitution pattern that, in turn, can be modified by chemical manipulation. Indeed, a large variety of BODIPY with a wide range of functional groups attached to the chromophore in all the available positions of the core may be found in the bibliography.

This review focuses on the possibility of tuning the photophysical properties of BODIPY dyes by modifying their basic molecular structure to develop new fluorophores with the emission shifted to the blue and red parts of the visible spectrum. Accordingly, the same laser dye family may cover completely the visible region by simply choosing the desired derivative.

To achieve the wanted red-shift of the spectral bands the delocalized π–system should be extended. This can be done in different ways: fusing aryl cycles, incorporating halogens of aromatic groups, or replacing carbons of the core by heteroatoms [70–74]. Here, we explore some of these possibilities.

The development of stable and efficient red dye lasers is of great interest in medicine and telecommunications. On the other hand, the development of blue–emitting laser dyes is somehow more troublesome. In the past, some attempts have been done, but failed in terms of fluorescence and lasing efficient [75–77]. Moreover, one of the major drawbacks of the available commercial blue dyes is their lack of stability. We have accomplished this type of dyes by the formation of hemicyanine–like structures upon amine substitution. Blue dye lasers have interest in microscopy and electroluminescent devices. Finally, we explore the use of halogenated BODIPY as singlet oxygen generators because of their potential use in photodynamic therapy [78–81]. The photophysical characterization of BODIPY derivatives has been complemented by quantum mechanics calculation results.

2. General Photophysics of BODIPY Dyes:

Figure 1 shows the UV/Vis absorption and fluorescence spectra of BODIPY chromophore. The lowest energy Vis absorption band, corresponding to the electronic transition from the ground to the first excited states ($S_0 \rightarrow S_1$ transition), is characterized by a high transition probability, with high molar absorption coefficient ($\varepsilon \sim 10^5\ M^{-1}\ cm^{-1}$) and oscillator strength ($f \approx 0.5$). It presents a shoulder at higher energies (at around 1100 cm^{-1} from the absorption maximum), which is attributed to out–of–plane vibrations of the aromatic skeleton. Other

absorption bands, corresponding to transitions to higher singlet excited states (S_2, S_3…), appear in the UV region and are less probable [82]. Quantum mechanical calculations suggest that the main absorption band corresponds to an allowed $A_1 \rightarrow B_2$ transition, according to a C_{2v} symmetry, with the transition dipole moment oriented along the longitudinal axis. Theoretical results indicate that this Vis band is assignable to the promotion of an electron from the HOMO orbital to the LUMO molecular orbital (Figure 1A), which is polarized along the long molecular axis of the chromophore [83].

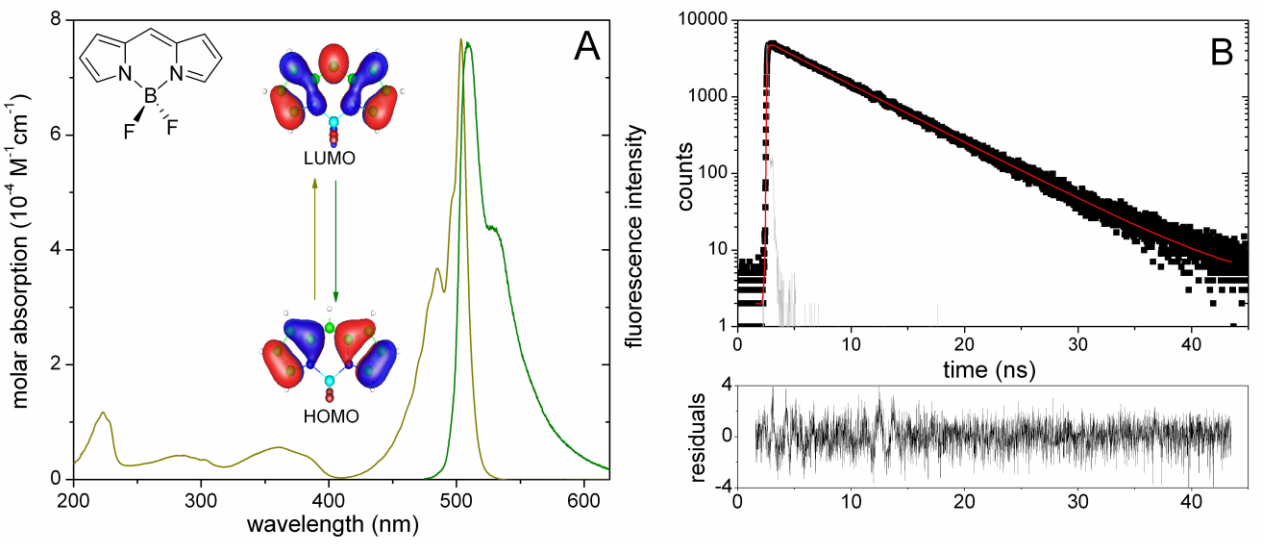

Figure (1): A) Absorption and fluorescence spectra of the BODIPY chromophore in a diluted solution of cyclohexane, together with its corresponding HOMO and LUMO contour maps. B) Fluorescence decay curve and the residuals from a monoexponential fit.

The shape of this absorption band is nearly independent of the dye concentration (at least up to 2×10^{-3} M) suggesting the absence of any intermolecular dye–dye interaction, including dye aggregation [9]. This low tendency of BODIPYs to self–associate is a very important advantage of these dyes with respect to other laser dyes, such as rhodamines, since the formation of non– or poorly fluorescent aggregates, drastically reduces the fluorescent capacity in concentrated solutions, generally required to record the laser signal [84].

The fluorescence spectrum of BODIPYs is practically the mirror image of the $S_0 \rightarrow S_1$ absorption band (Figure 1A), suggesting similar vibrational levels in both electronic states. Indeed, quantum mechanical calculations point out that the optimised geometry in the S_1 excited state is quite similar to that of the S_0 ground state. Consequently, the fluorescent band is characterized by a small Stokes shift (around 500 cm^{-1}). The shape of the fluorescence band is independent of the excitation wavelength indicating that the emission is from the lowest vibrational level of the S_1 excited state, independent of the electron–vibrational level directly populated in the excitation process [9]. Therefore, a very fast internal conversion process from upper excited states populates the fluorescent excited state. The fluorescence quantum yield (ϕ) can be very high, reaching values close to the unit for some BODIPYs in certain media [9].

Generally, the fluorescence decay curves of BODIPYs can be analyzed as monoexpoenential decays, with fluorescence lifetimes (τ) around 4–6 ns (Figure 1B). The lifetime is independent

of the excitation and the emission wavelengths, confirming the simple emission from the locally excited state.

The high fluorescence ability of BODIPY is a consequence of its chromophoric unit. The BF_2 group acts as a linking bridge, providing a rigid delocalized π–system. The BF_2 group does not participate in the aromaticity of the π–system but avoids any cyclic electron flow around the chromophoric ring [85]. Consequently, BODIPY dyes can be classified as quasi–aromatic dyes and are characterized by a low intersystem crossing probability by means of the "Drexhage's loop rule" [2]. This low population of the triplet state is a significant advantage for the potential application of BODIPYs in photonics since the triplet–triplet absorption, one of the most important losses in the resonator cavity, is drastically reduced. Therefore the non–radiative deactivation pathways are mainly controlled by internal conversion processes, which are related to the flexibility/rigidity of the molecular structure. In any case, and due to the rigidity and planarity of the chromophoric units (confirmed by quantum mechanical calculations and X–ray diffraction data [86]), the non–radiative deactivation of BODIPY dyes is expected to be low, in agreement with the experimental evidences for the high fluorescence ability of these dyes [87].

2.1. Alkyl Substitution Effect:

The experimental and theoretically predicted photophysical properties the BODIPY chromophore and their alkylated derivative (Scheme 1); PM546 [88], PM567 [82] and PM597 [89], are collected in Table 1. These dyes present methyl groups at 1, 3, 5, 7 and 8 positions of the chomophoric ring, whereas differ in their substitution at 2 and 6 positions (hydrogen, ethyl and *tert*-butyl, respectively in Scheme 1). The alkylation does not significant affect on the photophysics of BODIPY chromophore [82]. Just, a slight bathochromic shift of the absorption and fluorescence bands, but similar fluorescence quantum yields and lifetimes (Table 1). However, the presence of the *tert*–butyl groups (PM597) not only induces further bathochromic spectral shifts, mainly in the fluorescence band, due to its higher inductive electron donor ability, but also decreases (around a 50%) the fluorescence quantum yield and lifetime [89]. These results reveal an important Stokes shift (around 1300 cm^{-1}, among the highest reported for BODIPY) and a considerable increase in the non–radiative rate constant (k_{nr}) of PM597 with respect to the other alkyl derivatives (Table 1).

Table (1): Experimental (dye concentration 2×10^{-6} M in methanol) and theoretically predicted (TD–B3LYP in gas phase) photophysical properties of BODIPY chromophore and its alkylated derivatives PM546, PM567 and PM597: wavelength of absorption and fluorescence maximum (λ_{ab} and λ_{fl}), Stokes shift ($\Delta\nu_{St}$), molar absorption coefficient (ε_{max}), oscillator strength (f), fluorescence quantum yield (ϕ) and lifetime (τ), rate constants of radiative (k_{fl}) and non–radiative (k_{nr}) deactivation.

	Experimental				Theoretical			
	BODIPY	PM546	PM567	PM597	BODIPY	PM546	PM567	PM597
λ_{ab} (± 0.5 nm)	497.0	492.0	516.0	523.0	393.0	405	425	430
ε_{max} (10^4 M^{-1} cm^{-1})	5.8	8.2	7.9	7.6	–	–	–	–
f	0.36	0.40	0.49	0.38	0.42	0.53	0.54	0.52
λ_{fl} (± 0.5 nm)	507.0	504.0	531.5	561.0	397	410	435	455
ϕ (± 0.05)	0.87	0.95	0.91	0.48	–	–	–	–
τ (± 0.1 ns)	7.33	5.58	6.10	4.21	–	–	–	–
k_{fl} (10^8 s^{-1})	1.18	1.71	1.49	1.14	1.27	1.88	1.60	1.61
k_{nr} (10^8 s^{-1})	0.18	0.09	0.15	1.23		–	–	–
$\Delta\nu_{St}$ (cm^{-1})	395	455	560	1305	260	215	360	1365

The quantum mechanical simulation nicely reproduces the experimental photophysical properties trends. It was previously demonstrated that the absolute S_0–S_1 energy gap values proposed by semiempirical methods are closer to the experimental ones than those predicted by the TD–B3LYP method. Indeed, this DFT method overestimates this energy gap. However, the DFT method provides better values for the oscillator strength (f) and the radiative rate constant (k_{fl}) and reproduces more accurately the spectral shifts and changes in the transition moments of BODIPYs by the effect of the substituents and the solvent. For this reason, only the DFT results are enclosed in Table 1 [83, 90].

The observed bathochromic spectral shifts by the presence of alkyl groups are attributed to their inductive effect. For instance, upon substitution at positions 2 and 6, quantum mechanical calculations suggest a lower electron density at the 2 and 6 positions in the LUMO than in the HOMO state (see contour maps inserted in Figure 1). Consequently, the inductive effect +I of alkyl group at those positions would stabilize more extensively the LUMO S_1 excited state than the HOMO S_0 ground state, reducing the S_0–S_1 energy gap (spectral shift to lower energies). Accordingly, the incorporation of a more inductive electron donor group, as the branched *tert*–butyl group, leads to more extended shift to lower energies (Table 1) [89].

For PM597, the bathochromic shift in the fluorescence band is higher than in the absorption band giving rise to a large Stokes shift (Table 1). This observation could be indicative of a change in the geometry of this derivative upon excitation. This is confirmed by quantum mechanical calculations. Indeed, the pyrrole rings are not planar in the S_1 excited state of PM597 (dihedral angle of 4.7º) versus the nearly planar structure (dihedral angle around 0.2º) proposed for the pyrrole ring in the S_1 state of PM567. This distortion in the S_1 geometry has been attributed to the steric hindrance between the bulky *tert*–butyl groups with the adjacent methyl groups at 1– and 7–position of the PM597 core [89]. This loss in the planarity can be interpreted as a reduction in the rigidity of the chromophoric BODIPY system, favouring the internal conversion processes for PM597 and reducing its fluorescent capacity with respect to other BODIPY dyes with linear alkyl groups (Table 1).

2.2. Solvent and Polymer Solid Matrix Influence:

The photophysical properties of BODIPY dyes have been studied in a wide variety of apolar, polar and protic solvents [89]. Table 2 summarized the corresponding results for PM597 as a representative dye. Other alkyl–BODIPYs show similar qualitative tendencies [82,88]. In general, the spectral bands shift to higher energies and the fluorescent capacity and lifetime increase when apolar media are changed by polar/protic media. The augmentation in the fluorescence ability is due to a reduction in the non–radiative deactivation rather than to an enhancement in the radiative decay. All these experimental results have been confirmed by quantum mechanics where the solvent was simulated as a continuum medium [90].

The alternating electronic charge delocalisation through the conjugated π–system suggests that BODIPY dyes can be defined as cyclic polymethine– or cyanine–like structures [91,92]. The dipole moment, oriented along the short molecular axis due to symmetry reasons, is relatively low ($\mu \approx 3$ D in the ground state), making BODIPY dyes normally insoluble in water. Theoretical results suggest that the dipole moment slightly decrease upon excitation ($\Delta\mu = -1$ D in gas phase). Consequently, S_0 state would be more stable than S_1 one in polar solvents, giving rise to a moderate hypsochromic spectral shift with the solvent polarity, as is experimentally observed (Table 2).

Table (2): Photophysics of PM597 dye in diluted solutions (2×10^{-6} M) of several solvents

Solvent	λ_{ab} (nm)	ε_{max} ($10^4 M^{-1}cm^{-1}$)	λ_{fl} (nm)	ϕ	τ (ns)
2–methylbutane	527.1	8.20	569.0	0.40	4.19
hexane	527.5	8.25	567.8	0.43	4.35
c–hexane	529.0	8.10	571.2	0.32	3.91
isooctane	527.5	8.05	569.0	0.40	4.43
diethyl ether	525.1	7.90	565.4	0.43	4.27
1,4–dioxane	525.1	7.85	565.4	0.40	4.37
THF*	525.1	7.75	566.6	0.37	4.15
DMF*	524.0	5.89	565.4	0.35	4.69
acetone	522.5	7.44	563.6	0.44	4.34
2–pentanone	523.7	6.13	562.6	0.46	4.54
methyl formate	522.3	7.55	560.6	0.47	4.45
methyl acetate	522.5	7.85	561.8	0.48	4.44
ethyl acetate	523.2	7.67	562.4	0.44	4.31
buthyl acetate	524.3	7.85	564.6	0.43	4.51
acetonitrile	520.8	7.60	560.6	0.44	4.27
1–octanol	527.3	7.70	565.0	0.41	4.68
1–hexanol	526.7	7.55	565.4	0.42	4.59
1–butanol	526.1	7.70	566.6	0.39	4.33
1–propanol	525.3	7.75	564.6	0.39	4.19
ethanol	524.3	7.63	563.2	0.43	4.09
methanol	522.9	7.58	561.2	0.48	4.21
F3–ethanol*	521.6	7.01	561.2	0.49	4.64

*DMF=dimethylformamide, THF=tetrahidrofurane,
F3-ethanol=2,2,2–trifluoroethanol

An accurate understanding of the solvent effect can be achieved by a multilinear correlation analysis [93–95]. This method simultaneously correlates a physicochemical property (XYZ) with different solvent parameters (A, B, C, ..) by means of :

$$(XYZ) = (XYZ)_o + c_A A + c_B B + c_C C + \ldots.. \quad (1)$$

where $(XYZ)_o$ is the physicochemical property of interest in an inert solvent and c_A, c_B, c_C, … are the adjusted coefficients, which reflect the dependence of the physicochemical property on the corresponding A, B, C,…. solvent parameters.

The photophysical properties of aromatic system are generally correlated with the solvent polarity/polarizability, H–bond donor/acceptor capacity and electron releasing ability [91]. Among the different solvent scales proposed in the bibliography we have chosen those derived by Taft; π*–, α– and β–scales, respectively [96–98]. Figure 2 shows the evolution of the experimental absorption and emission maxima (ν_{ab} and ν_{fl} in cm^{-1}) of PM597 with those predicted by the above linear regression (eq. 1). The relative low correlation coefficient ($r < 0.9$) is due to the relative low spectral shifts observed for PM597 from apolar to very polar/protic solvents (not more than 10 nm). Experimental results suggest that the absorption and fluorescence bands of PM597 are mainly affected by the solvent polarity/polarizability (high c_{π^*} values), although the electron release capacity of the solvent can also affect, in some extent, on the band position. In general absorption and fluorescence bands shift to higher energies by increasing the solvent polarity/polarizability ($c_{\pi^*} > 0$), while the solvent basicity induces slight spectral shifts toward lower energies ($c_\beta \leq 0$). The effect of the solvent acidity on the spectral positions is practically neglectable ($c_\alpha \approx 0$), mainly in the absorption band.

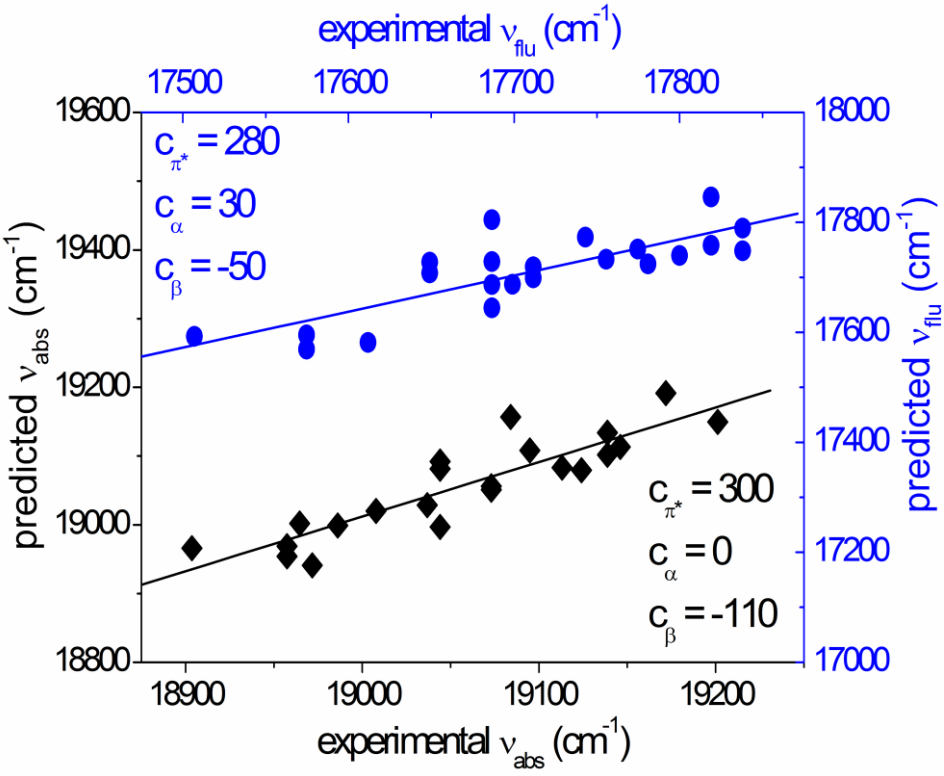

Figure (2): Multilinear regresión analysis of the absorption and emission wavelength for the PM597 by means of the Taft solvent scales. Enclosed the corresponding adjusted coefficients for the solvent polarity/polarizability (π^*), acidity (α) and basicity (β).

An alternative method to analyze the solvent effect on the spectroscopic parameters is by means of a linear relationship between a physicochemical properties (XYZ) and a multicomponent solvent parameter (M), eq.(2), in which several solvent properties are included [94].

$$(XYZ) = (XYZ)_o + c_M M \qquad (2)$$

For instance, the Reichardt $E_T^N(30)$ is a very popular multicomponent solvent parameter in which both solvent polarity/polarizability and H–bond capacities are included [99].

The observed increase in the ϕ and τ values of PM597 with the solvent polarity (Table 2), is mainly due to a decrease in the k_{nr} rate constant rather than to an increase in the k_{fl} value which is observed to be nearly solvent independent. Figure 3 shows the evolution of the k_{nr} value (in logarithm scale) of PM597 with the $E_T^N(30)$ solvent parameter. The good linear relationship (r = 0.85–0.90) suggest the validity of eq.(2) applicable, in this case, for the non–radiative deactivation rate constant of PM597. The reduction of the internal conversion in polar/protic solvents could be due to a diminution of the electron flow as a consequence of a restriction in the delocalisation of the positive charge through the π–system of the BODIPY chromophore [86]. Previous works of rhodamines and coumarins demonstrated that those factors favouring the movement of the positive charge through the delocalized π–system can be look as a loss in the rigidity of the chromophoric system and hence to a decrease of the fluorescence ability [100]. Thus, an electrostatic stabilization of the positive charge with the dielectric constant of the solvent or any specific solute–solvent interaction reducing the charge mobility through the conjugated π–system, should lead to a diminution in the non–radiative deactivation. Similar arguments can be applied for the case of other alkyl–BODIPY dyes [9].

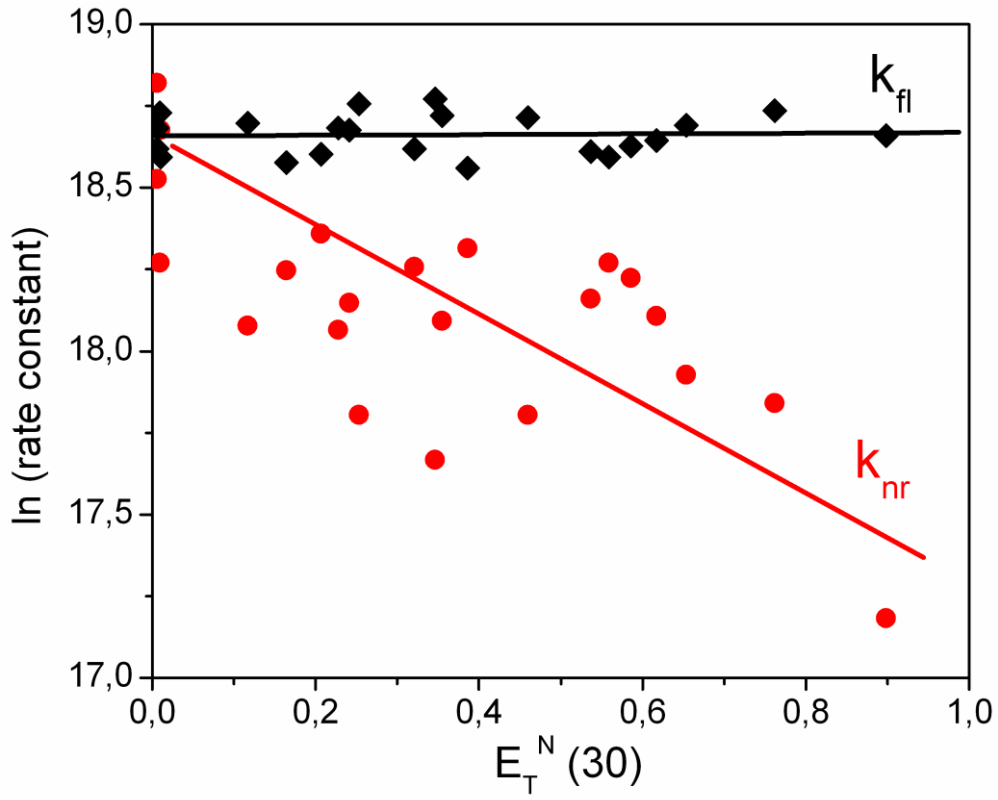

Figure (3): Correlation between the non–radiative (k_{nr}) and raditive (k_{fl}) rate constant of PM597 with the normalized Reichardt parameter ($E_T^N(30)$).

In the introduction section we have pointed out the key role of the photophysical properties in order to understand the lasing action. Indeed, a good correlation is established between the photophysical properties and the lasing characteristics of alkyl–BODIPYs by changing both the molecular structure of the dye (substituent effect) and the solvent (Figure 4) [9]. Thus, similar bathochromic spectral shifts are observed in the fluorescence and lasing band by the incorporation of ethyl (PM567) or *tert*–butyl (PM597) groups at the 2– and 6–positions of PM546 or changing from a polar/protic solvent to an apolar environment for a common alkyl–BODIPY dye (PM546, PM567 or PM597). Similar correlation can be also established

between the lasing efficiency and the fluorescence capacity by changing both the molecular structure of the dye and the environmental conditions of the surrounding media.

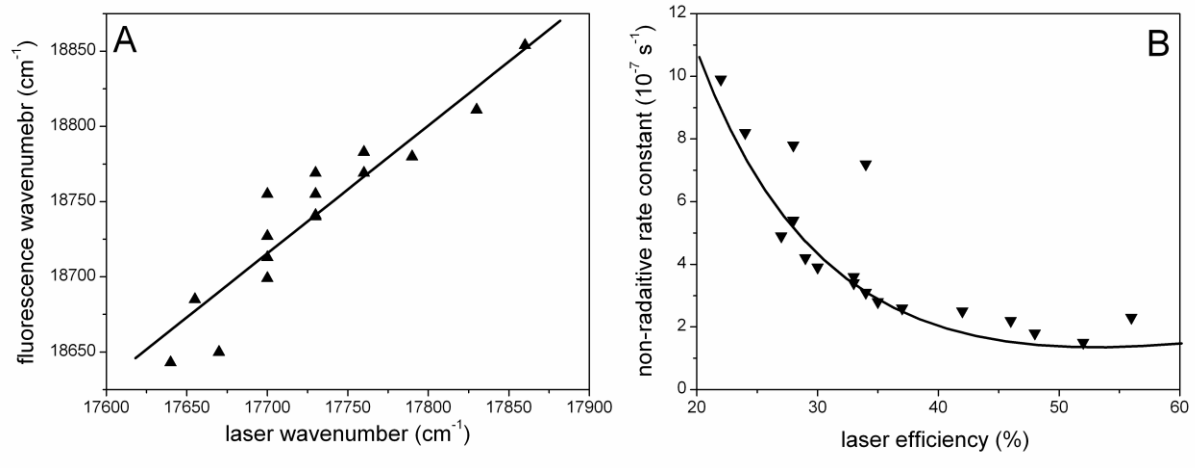

Figure (4): Correlation between the fluorescence and the laser characteristics of PM567: (A) band position (in wavenumbers) and (B) non−radiative rate constant and laser efficiency.

One of the most active research areas is focused on the developments of solid−state dye lasers. Solid state devices have inherent technological advantages such as the compactness, the absence of toxic and inflammable solvents, etc. In these lasers, the dye is embedded into a transparent solid host material, which can be of both organic and inorganic nature [8]. Inorganic materials generally improve the mechanical and thermal stability of the active media, whereas organic materials favour the chemical compatibility between the host and the guest materials. One of the most commonly used organic host matrices are polymer systems. Concretely, polymethylmethacrylate (PMMA) has been largely used as organic host material because of the nice optical homogeneity and the viscoelastic properties and polarity of the polymer can be controlled by the synthesis conditions [101].

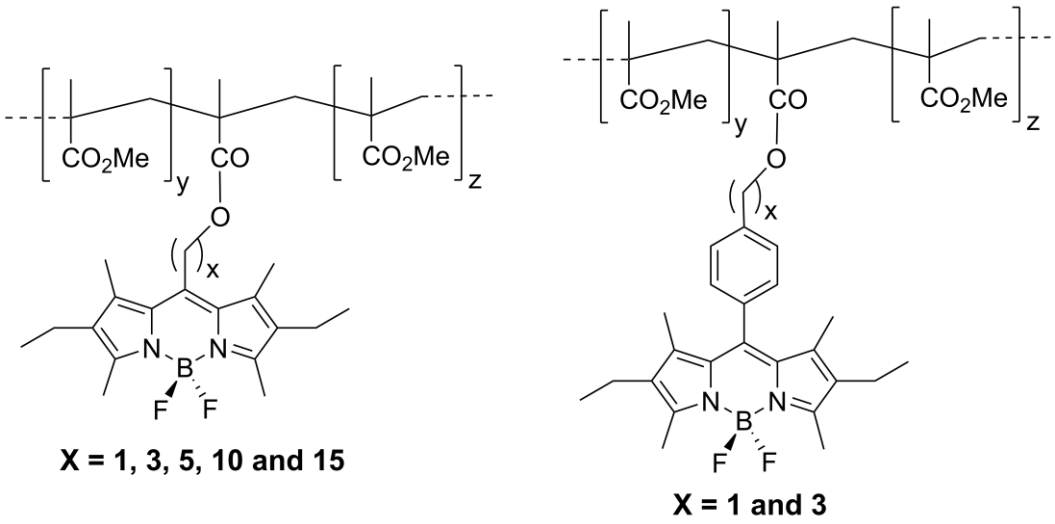

Scheme (2): Covalent linkage of the PM567 to the polymeric chain change through a phenyl spacer and a polymethylene chain of different length.

Alkyl−BODIPY dyes have been incorporated into PMMA matrices, both as dopant and covalently linked to the polymer chain (Scheme 2) [102−106]. From the experimental studies

performed in solution it seems that the structural or environmental rigidity, as well as the solvent polarity, enhances the fluorescence capacity of BODIPYs. In PMMA, the elasticity/rigidity of the solid matrix can be modified by the copolymerization of MMA with adequate crosslinking agents [107], while the polarity can be incremented incorporating fluorinated–MMA comonomers [106]. Finally, the BODIPY dye can be covalently linked to PMMA chains can be performed through spacers (polymethylene chain (–(CH_2)n–) of different length (n = 1, 3, 5, 10 and 15 methylene units) or a *para* substituted phenyl group (Scheme 2) [102,103,105].

In general, the experimental the absorption and fluorescence bands almost do not shift with the solid matrix (similar λ_{ab} and λ_{fl} values are obtained in pure solid PMMA and in liquid ethanol, a solvent which can mimetic the physicochemical properties of MMA). However, the fluorescence ability of the BODIPY depends on the type and extent of the crosslinking comonomers [104]. Indeed, in concordance with the lasing measurements [107], the fluorescence quantum yield reaches a maximum (Figure 5) which depends on the nature of the crosslinking agent (around 10% for TMPTMA and around 1% for PETRA). The different optimal crosslinking degree depending of the copolymer has been related to the glass transition temperature (T_g) [107]. The T_g value of acrylic crosslinker is lower than that of the methacrylic one, providing a less rigid environment in the former case for the same crosslinking degree. A further increase in the crosslinking degree beyond this optimal point reduces the fluorescence capacity, probably because an excessively rigid environment damages the dye.

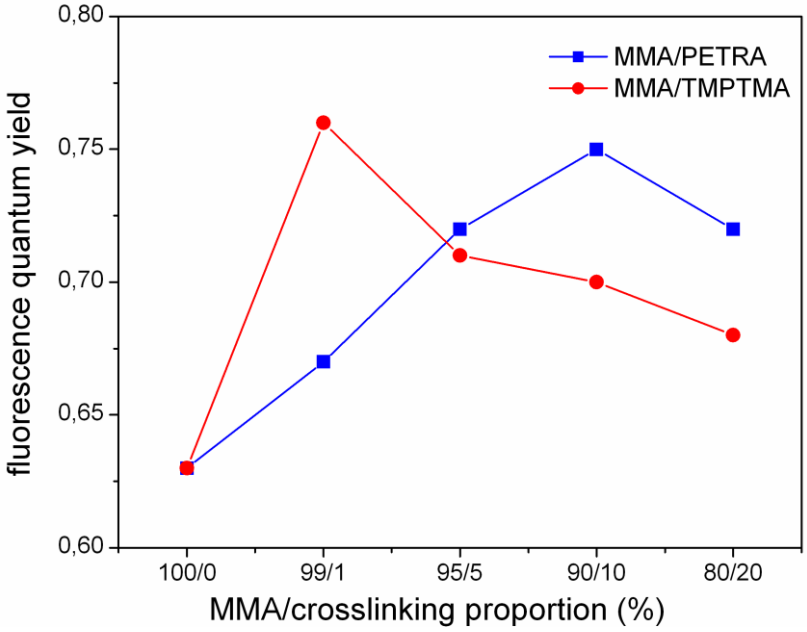

Figure (5): Evolution of the fluorescence quantum yield of PM567 with the crosslinking (PETRA or TMPTMA) content in the polymeric matrix.

On the other hand, the combination of crosslinked matrices with fluorinated monomers should be beneficial for the fluorescence efficiency and hence for the lasing action [106]. In this case, we try to take advantage of the two factors which ameliorates the fluorescence capacity; a more constrained and polar environment [9]. As expected, the fluorescence efficiency increases in fluorinated matrices with respect to in the homopolymer PMMA (Figure 6). This increase correlates with a similar augmentation observed in the fluorescence lifetime, suggesting a reduction in internal conversion processes of PM567. This diminution in the k_{nr} value agrees with that observed in liquid solution (F_3–ethanol in Table 2). Even more, a

further increase in the fluorescence capacity is observed when crosslinker monomers are also included in the fluorinated matrices (Figure 6). In the case of PM597 dye, the effect of the solid polymeric matrices is more pronounced. This dye presents higher fluorescence quantum yields and lifetimes in solid polymers ($\phi \approx 0.5–0.6$ and $\tau \approx 7–8$ ns) than in liquid solutions ($\phi \approx 0.4–0.5$ and $\tau \approx 4.0–4.5$ ns). As is discussed above, the internal conversion of PM597 is higher than other alkyl–BODIPY dyes due to a loss in the planarity of the chromophoric ring in the excited state [89]. Such a geometrical change could be reduced in the rigid environment provided by the polymeric matrices, improving the fluorescence capacity of this dye in solid materials. Moreover, the fluorescence capacity of PM597 progressively increases with the polarity and rigidity of the copolymer (Figure 5), with a similar evolution to that observed for PM567. In the case of PM597 dye, the beneficial effect of the rigidity and polarity of the solid polymeric matrix is more pronounced and the dye presents even higher fluorescence quantum yields and lifetimes in solid polymers ($\phi \approx 0.5–0.6$ and $\tau \approx 7–8$ ns) than in liquid solutions ($\phi \approx 0.4–0.5$ and $\tau \approx 4.0–4.5$ ns). As is discussed above, the internal conversion of PM597 is higher than other alkyl–BODIPY dyes due to a loss in the planarity of the chromophoric ring in the excited state [89]. Such a geometrical change could be reduced in the rigid environment provided by the polymeric matrices, improving the fluorescence capacity of this dye in solid materials.

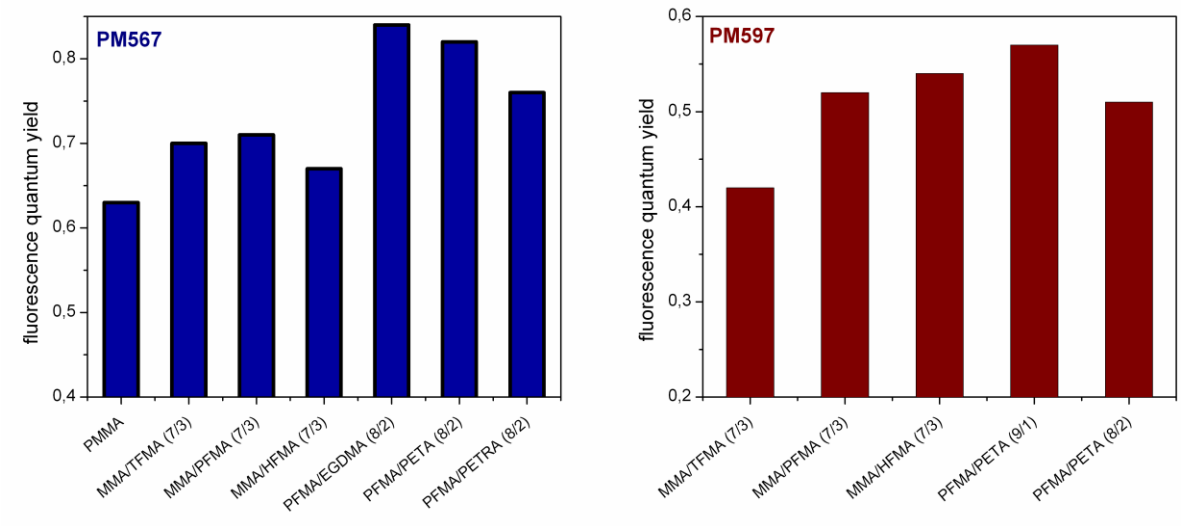

Figure (6): Evolution of the fluorescence quantum yield of PM567 and PM597 with the fluorination and crosslinking degree of the polymer.

Finally, the covalent linkage of the BODIPY to the polymeric chain through its *meso* position by means of a long enough (polymethylene chain with more than three units) or phenyl space (Scheme 2) does not alter the photophysics of the dye, being very similar to the respective dyes incorporated in PMMA as dopants [102,105]. However, when the spacer is short the proximity of the methacryloyloxy group decreases the fluorescence capacity decreases, due to a decrease of the radiative rate constant, and the spectral bands shifts to lower energies. Probably, the inductive electron withdrawing character of the substituent reduces the aromaticity of the electronic π–system of the chromophore, leading to a diminution in the radiative deactivation probability and an augmentation in the $S_0–S_1$ energy gap [108]. The phenyl spacer has nearly negligible influence because group acts as a spacer between the polymer chain and the dye, the photophysical properties of BODIPYs are practically unaltered because is disposed practically perpendicular to the BODIPY core, avoiding any resonant interactions between the electronic clouds of both entities, as revealed by quantum

mechanical calculations [87, 103]. This perpendicular arrangement is assigned to the steric hindrance between the *ortho* H–atoms of the phenyl group and the adjacent methyl groups at the 1– and 7–position of the BODIPY core.

Although the covalent binding by long enough chains or phenyl group dos not imply an extra improvement nor in the fluorescence neither in the lasing efficient [102,105], such covalent linkage considerably enhances the thermostability of the BODIPY chromophore, probably because the chemical linkage provides extra pathways to the dye to eliminate the excess of heat accumulated during the laser action [102]. This fact is a great advantage to develop solid state dye lasers, because the thermal degradation is one of the most important reasons for dye damage [8]. In this way, the operative lifetime of the active media can be considerably increased by the covalent linkage.

Summing up, photophysical measurements and quantum mechanical calculations are crucial to find the structural and environmental conditions which optimize the lasing performance of alkyl–BODIPY dyes and to understand their lasing performance. Furthermore, a careful control of the photophysics of the BODIPY just by the attachment of adequate functional groups allows spanning their spectral region action or applying them in novel fields of interest.

3. Blue–emitting BODIPYs:

The development of blue-emitting devices is of great interest not only from a technological point of view, for data storage and displays, but also in chemical and biological research in microscopy, sensing and photo/electroluminescent devices [109–115]. Most of the commercially available blue laser dyes are not optimal for lasing applications because show low lasing efficiency and fast photobleaching. One way to circumvent such lack of efficiency and stability is to make use of the robust BODIPY dye. However, the shift of their emission bands to the blue is not an easy task. In the past, some attempts have been made to this aim strongly modifying the chromophoric core [75–77]. Thus, dinitrogen-BF_2 compounds analogous to the BODIPY were developed where the dipyrrol core were replaced by anthracene, cyclopentalene or fluorene and even adding N atoms to the heterocyclic. However, poor results were obtained from a fluorescence and lasing point of view, with the exception of the derivative consisting in an aza-anthracene like chormophore [77]. In the present chapter, we present a straightforward method to achieve blue-emitting BODIPY dyes without drastically alter the chromophoric core, just adding amino group to the *meso* position (Scheme 3) [116,117].

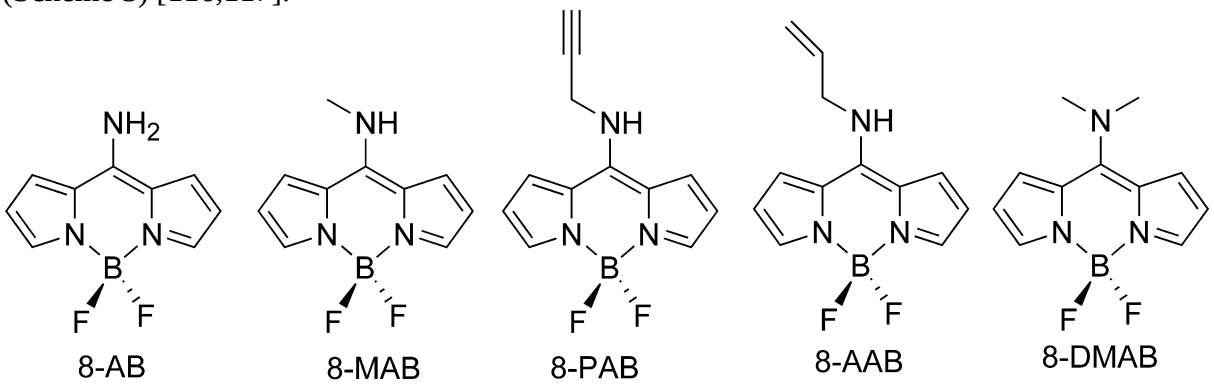

Scheme (3): Molecular structure of the 8–amino substituted BODIPYs.

BODIPY dyes bearing amino groups at *meso* position give rise to spectral bands in the blue part of the visible spectrum, as is illustrated in Figure 7. At a first sight, the electron pair localized at the amine should be susceptible to delocalization onto the BODIPY core and, as consequence, a red shift should be expected in terms of the resonant effect. However, in the present case the spectral bands are largely hypsochromically shifted (up to 100 nm) with respect to the reference unsubstituted BDP dye. Theoretical simulation also predicts an important hypsochromic shift of the spectral bands by the presence of the amine groups [117]. Regardless of the nature of the amine group, the absorption electronic transition is attributed to a promotion of an electron bands from the HOMO to the LUMO state, without any interference of lower occupied or higher virtual molecular orbitals. Therefore, the evolution of the energy of these frontier orbitals with the type of amine attached to the BODIPY core can be used to explain the spectral blue shift.

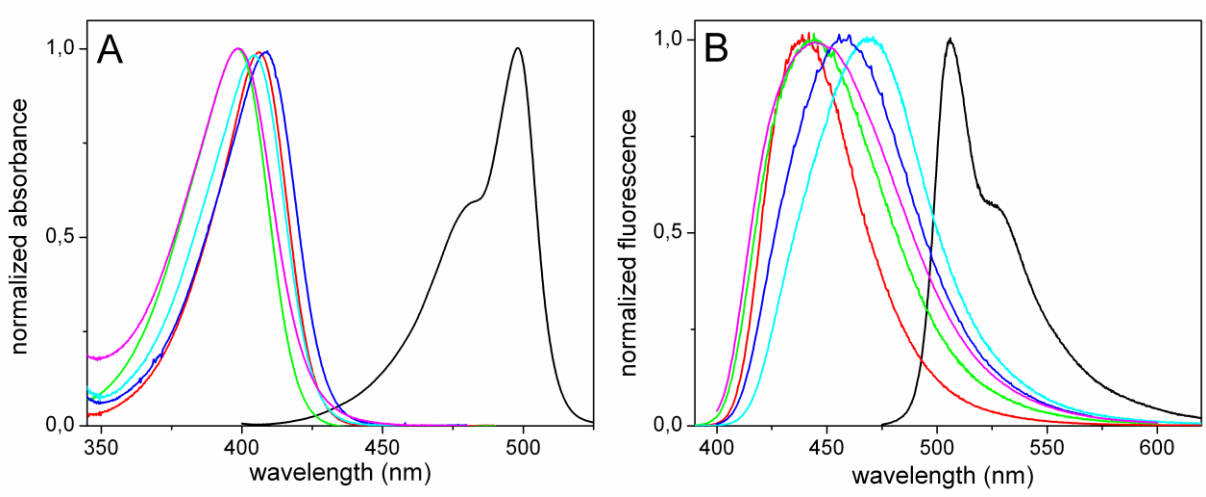

Figure (7): Normalized absorption (A) and fluorescence (B) spectra of BODIPY chromophore (black) and its 8-amino derivatives in ethyl acetate; 8–AB (red), 8–MAB (green), 8–AAB (blue), 8–PAB (cyan) and 8–DMAB (purple).

Indeed, quantum mechanical calculations suggest that the spectral shift is due to an increase of the energy of the LUMO state, while the HOMO energy remained unaltered (Figure 8 and Table 3). Previous work has shown that the position 8 of the BODIPY core is very sensitive to the substituent effect [9]. In fact, the electronic density in such position drastically increases from the HOMO to the LUMO state. The amine group is characterized by an electron donor character as reflected by its value in the Hammet scale (σ) accounting for the inductive field and resonant effects. Among the different Hammet parameters proposed we have chosen the σ_{p+}, better suited to describe a substituent effect in systems where a positive charge is delocalized through the aromatic framework [118], as is the case of BODIPY dyes (Table 3). Thus, the presence of such electron donor amine group at *meso* position induces a net destabilization of the LUMO state due to its high electronic density at that position.

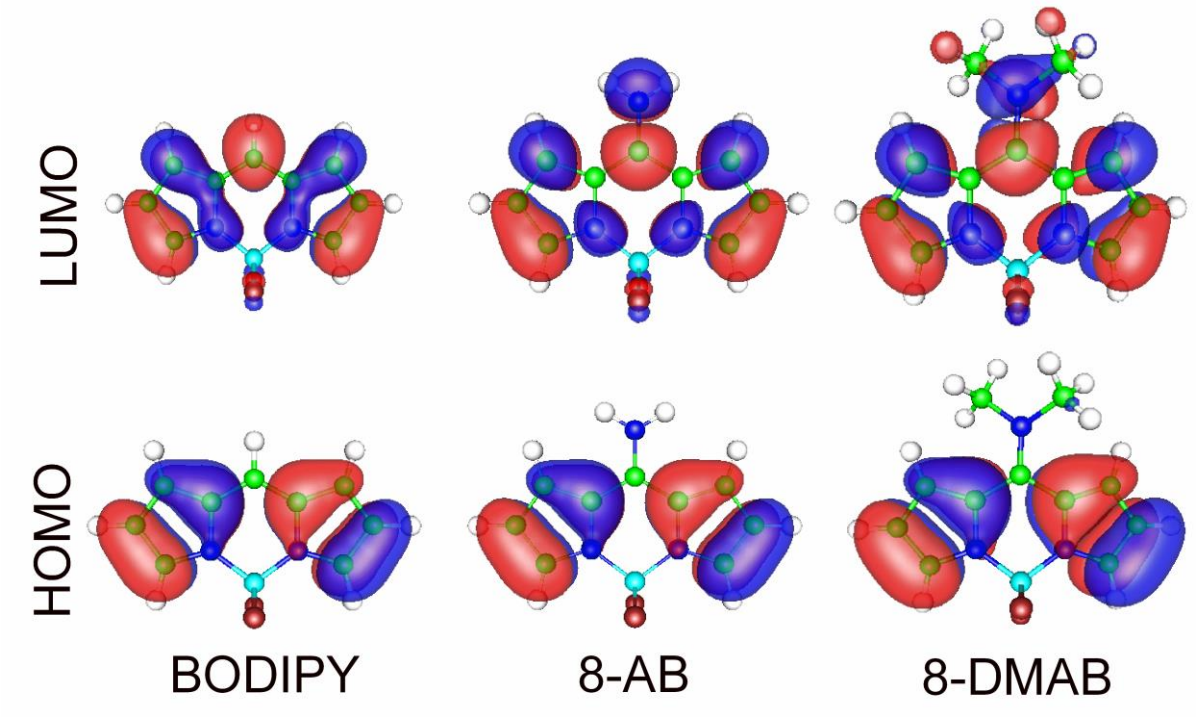

Figure (8): HOMO and LUMO contour maps of the BODIPY chromophore and its derivatives with a primary (8–AB) and tertiary (8–DMAB) amine at 8 position.

Table (3): Calculated energies (in eV) of the HOMO and LUMO frontier orbital of BODIPY and its 8–amino derivatives. The corresponding Hammet parameters (σ_p^+) accounting for the electron donor ability of the amine are also included for the primary amine, and the mono and dimethylated ones.

	E_{HOMO}	E_{LUMO}	σ_p^+
BODIPY	-6.095	-3.102	0
8–AB	-6.069	-2.421	-1.30
8–MAB	-5.985	-2.285	-1.81
8–AAB	-5.986	-2.285	-
8–PAB	-6.041	-2.367	-
8–DMAB	-5.959	-2.258	-1.70

Entirely opposite trends were registered upon substitution with the same amino but at 3 position of the BODIPY core. In this case, the amino group nearly did not affect the position of the spectral bands [119]. In fact, the HOMO and LUMO contour maps show similar electronic density at position 3 (Figure 8). Therefore, both states are equally affected by the amine group and the energy gap remains unaltered. Moreover, the presence of an electron withdrawing substituent as the cyano group, at the *meso* position, leads to an important bathochromic shift of the spectra bands [120]. In such case, the electron removal effect of the cyano group induces a net stabilization of the LUMO orbital, relaxing the high electronic density at position 8, which leads to a decrease of the energy of the LUMO state and consequently of the energy gap. All these results highlight the importance of both the electronic character of the substituent and the position of the BODIPY core in which they are attached. Thus, appropriate election of the substituent (electron donor or electron withdrawing, controlled by the Hammet parameter) and its position on the BODIPY core (based on the change of the electronic density between the HOMO and LUMO states) allow

obtaining blue or red shifted spectral bands with different displacement. In this way, the position of the spectral bands can be modulated, covering nearly the whole visible spectrum with the same laser dye family.

The blue shift obtained by the presence of the amino group at 8 position of the BODIPYs can also be interpreted in terms of the resonant structures depicted in Figure 9 [116,117]. The presence of the amino group should imply a rearrangement of the chromophoric π–system of BODIPY core, which is normally described as a cyclic cyanine (structure A). Thus a new resonant structure B, characterized by a hemicyanine–like delocalyzed π–system, should acquire a higher statistical weight [121–123]. In order to such electronic coupling take place, both, the amine and the BODIPY, should be coplanar. This new rotamer is characterized by the splitting into two entities: the pyrrole ring and the amino–methylenepyrrole system, being this last form (hemicyanine) the responsible for the hypsochromic shift, because of a shorter delocalize π–system.

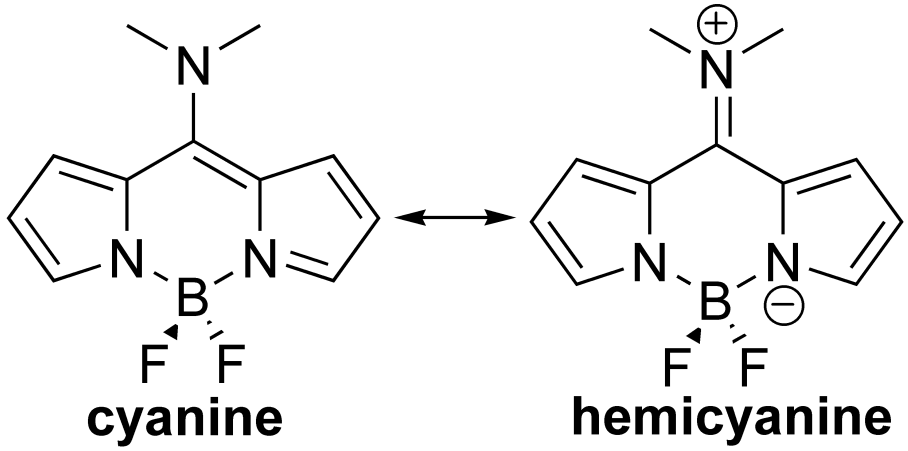

Figure (9): 8–amino BODIPYs rotamers.

On the other hand, electronic excitation leads to an increase of the negative charge on the amino group (Mulliken charges from –0.8 to –1.0), suggesting that the resonant structure A has a higher statistical weight in the excited state, whereas the B form in the ground state. In fact, the theoretical C–N bond length increases upon excitation (from 1.356 to 1.371), indicating a decrease of the bond order and confirming that the structure A is more important in the excited state. These features also explain the higher hypsochromic shift of the absorption band with respect to the fluorescence spectrum. Consequently, all the new amino–BODIPYs are characterized by high Stokes shifts (2000–4000 cm^{-1}), a desirable property in order to improve the emission efficiency of laser dyes by decreasing the reabsorption and reemission phenomena.

Table (4) summarizes the main photophysical data of the novel 8–amino–BODIPYs in solutions of different characteristics. These amino derivatives have a poor solubility in apolar media but are soluble in water (at least at low concentrations), a solvent in which BODIPYs are not commonly dissolved. This fact could be related to an increase of the dipole moment induced by the amino group. Their spectral bands are wider and exhibit lower vibrational resolution than those of the fully unsubstituted BODIPY (Figure 7), probably due to the above commented rearrangement of the aromatic π–system. Indeed, in all amino–BODIPYs the molar absorption coefficients are lower although the oscillator strengths are similar to those recorded to the BDP (Table 4). Both the excitation and fluorescence spectra are independent

of the emission and excitation wavelength, respectively, indicating that there is only one emitting entity. Since the influence of the electron donor strength of the amine substituent is an important parameter to take into account, we will focus on the effect of the amine group substitution pattern onto the photophysics of the BODIPY core.

Table (4): Photophysical data of BODIPY dye and its 8–amino derivatives in ethyl acetate and methanol.

	l_{abs} (nm)	e_{max} (f) ($10^4 M^{-1}cm^{-1}$)	l_{fl} (nm)	f	t (ns)	k_{fl} ($10^8 s^{-1}$)	k_{nr} ($10^8 s^{-1}$)	Dn_{St} (cm^{-1})
Ethyl acetate								
BDP	498.0	5.9 (0.38)	507.5	0.93	6.90	1.35	0.10	375
8-AB	406.0	2.9 (0.27)	444.0	1.00	4.25	2.35	0.00	2110
8-MAB	398.5	3.1 (0.34)	444.5	0.42	2.04	2.06	2.84	2595
8-PAB	408.5	3.3 (0.35)	469.5	0.94	5.13	1.83	0.11	3180
8-AAB	405.0	3.0 (0.32)	459.5	0.72	3.59	2.00	0.78	2930
8-DMAB	399.0	2.9 (0.35)	444.5	0.27	1.95	1.38	3.74	2565
Methanol								
BDP	497.0	5.8 (0.39)	507.0	0.87	7.33	1.18	0.18	395
8-AB	399.0	2.6 (0.26)	437.5	0.92	4.39	2.09	0.18	2205
8-MAB	394.5	3.0 (0.33)	440.0	0.10	0.52*	1.92	17.31	2620
8-PAB	405.0	3.3 (0.35)	464.5	0.52	3.22	1.61	1.49	3165
8-AAB	401.0	2.9 (0.31)	453.0	0.19	0.54*	3.52	15.00	2860
8-DMAB	396.0	2.7 (0.32)	438.0	0.09	0.50*	1.80	18.20	2420

*main component of the biexponential fit (contribution higher than 90%) and the one used to calculate the rate constants.

3.1 Amine Substitution Effect. Intramolecular Charge Transfer:

The presence of the electron donor primary (NH_2) amine group (σ_{p+} = –1.30), to yield the 8–AB dye, induces an important hypsochromic shift of the spectral bands, mostly in the absorption spectrum (Figure 7). In spite of its lower absorption probability, this dye is characterized by a very high fluorescence quantum yield (≈ 0.90–1.0) regardless of the environment properties (Table 4). The hypsochromic spectral shift of 8–AB with the solvent properties is more sensitive than that observed for normal alkyl–BODIPYs [9], probably related to specific interactions, like H bonds between the electron lone pair of the amine group and solvents. Considering all these features, it can be concluded that the 8–AB dye is highly suitable to be used as the active media of novel blue emitting tunable dye lasers.

On the other hand the amine monosubstitution (secondary amines) controls its electron releasing ability and hence its influence in the photophysics of the BODIPY. Indeed, methylation (8–MAB) increases the electron donor capacity of the amine group (σ_{p+} = –1.81), which leads to a higher instability of the LUMO orbital, increasing the energy gap and hence the hypsochromic shift of the absorption band (Figure 8 and Table 3). Besides to the reduction

of the absorption probability ($\varepsilon \approx 3\times10^4$ $M^{-1}cm^{-1}$), a decrease of the fluorescence capacity of 8–MAB is observed, being even clearer in polar media ($\phi \approx 0.15$), due to a drastic enhancement of the non-radiative deactivation processes (Table 4). Moreover, Figure 10 shows that in more polar solvents the fluorescence decay curve becomes biexponential owing to the appearance of a main short lifetime (500–700 ps). The other decay component matches that recorded from a monoexponential fit in apolar media (≈ 4 ns), but now, in polar solvents, with minor presence. Taking into account these experimental features and that methylation increases the electron donor ability of the amine, is probable that a non-fluorescent intramolecular charge transfer state (ICT) takes place [124]. Since no new absorption bands are observed at lower energies, such ICT state should be populated from the locally excited state (LE), and efficiently quenches the fluorescence emission, especially in polar media, where the ICT state is further stabilized. Besides, no new emission bands are detected at lower energies indicating that this ICT state is non-fluorescent. Furthermore, the dependence of the photophysics of the dye on the acidity of the media seems to confirm this hypothesis; in acid media, like 2,2,2–trifluoro–ethanol (Taft's polarity scale $\pi^* = 0.73$ and acidity scale $\alpha = 1.51$), the fluorescence quantum yield ($\phi = 0.23$) and lifetime ($\tau = 1.42$ ns) increase with respect to the values recorded in other polar solvents like water ($\pi^* = 1.09$ and $\alpha = 1.17$, $\phi = 0.06$ and $\tau = 0.28$ ns). The protonation of the amine group decreases the electron donor character of the amine and hence the formation of the ICT state.

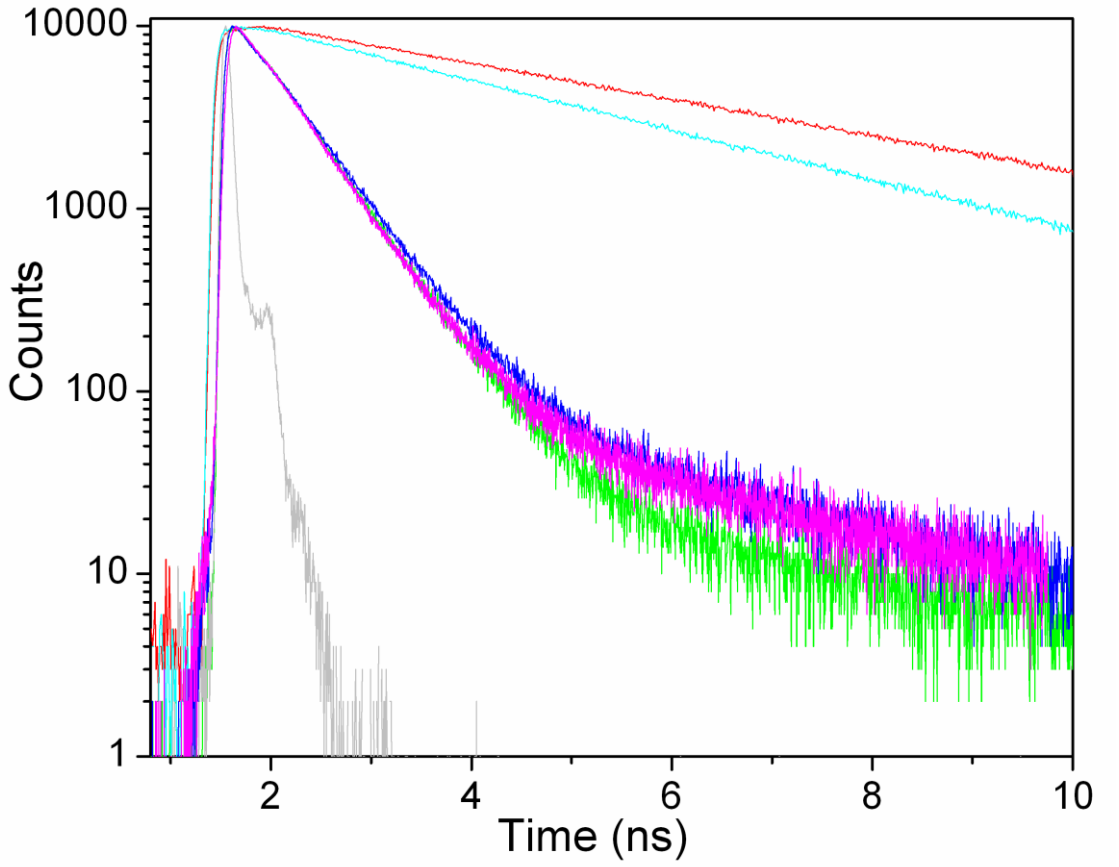

Figure (10): Fluorescence decay curves of the 8-amino derivatives in methanol; 8–AB (red), 8–MAB (green), 8–AAB (blue), 8–PAB (cyan) and 8–DMAB (purple).

Among the secondary amines, allyl (8–AAB) and propargyl (8–PAB) substituents have been also considered. The expected blue shift of the absorption band was also observed with respect to the fully unsubstituted BDP dye but in lower extension than the registered for

8–MAB counterpart (Figure 7). In fact, the blue shift follows the sequence: λ(8–MAB) < λ(8–AAB) < λ(8–PAB). Moreover, the fluorescence capacity follows a reverse order, being 8–PAB the best dye and 8–MAB the worse one. The double bond of the allyl, as well as the triple bond of the propargyl, is too far away from the BODIPY core to interact by resonance. Nonetheless, the presence of such unsaturations modifies the electron donor character of the amine being lower with the allyl moiety, and even lower with the propargyl group, than with the methyl one. Therefore, there should be a direct relationship between the electron donor capacity of the amine and the extent of the blue shift of the spectral bands. Previously, the blue spectral shift was explained on the basis of the destabilization of the LUMO state by the electron releasing effect of the amine substituent. Thus, amines with different electron donor strength should increase the LUMO energy to a different extent, modulating the increase of the energy gap. Moreover, such electron donor ability is closely related to the formation of the ICT state, and hence to the fluorescence capacity of the dye.

Briefly, the higher the electron donor strength capacity of the amine substituent, the higher the spectral hypsochromic shift, but the lower the fluorescence ability, due the formation of the quenching ICT state. The dependence of the fluorescence ability on both the amine group substitution pattern and the solvent polarity confirm the presence of the ICT state, which formation and stabilization should control the lasing performance of these amino–substituted BODIPYs. Indeed, apolar media, which reduce the probability of the fluorescence quenching through this ICT process, are the most recommended environments to optimize the lasing action.

Finally, the disubstitution of the amine (tertiary amine) was also considered**.** At first sight, it should be expected that the amine derivative bearing two methyl groups (8–DMAB) induces a longer blue shift of the spectral bands than that observed for all the above commented amino-BODIPYs. However, the Hammet parameter for the dimethylamine group (σ_{p+} = –1.70) is similar to that of the monomethylated one (σ_{p+} = –1.81). Experimental findings are well correlated with these parameters. Indeed, the spectral blue shift for 8–DMAB dye is similar to that induced for 8–MAB derivative (Figure 7). The fluorescence quantum yield and lifetime are similar for both dyes, indicating that the probability of formation of the ICT state is nearly the same (Table 4). Therefore, both methylated dyes (8–MAB and 8–DMAB) are the ones absorbing and emitting deeper in the blue region of the visible but with the lower fluorescence efficiency, which could reduce their potential laser action.

Another evidence that the ICT process should be responsible for the optical properties exhibited by these new 8–amino BODIPY derivatives is provided by the ionization potentials of the amino substituents, which account for their electron releasing ability. Although some of these ionization potential values can be extracted from the literature, we have theoretically calculated all of them from their HOMO energies (Table 5) in order to carry out a proper comparison with the trend suggested by the Hammet parameters. The probability of the presence of an ICT process is expected to increase as the ionization potential of the amino substituent decreases. According with the calculated data, the ionization potentials follow the order: NMe_2 < NHMe < $NHCH_2CHCH_2$ < $NHCH_2CCH$ < NH_2, which is the same order in which the fluorescence quantum yields of the new dyes decrease. Consequently, the discussion of the optical properties of the new dyes from the ionization potentials confirms the behavior suggested by the Hammet parameter about the amino group effect in both the band positions and the probability of formation of the intramolecular charge transfer state.

Table (5): Experimental and theoretically calculated ionization potentials (in eV) of the amine substituents in the blue–emitting BODIPYs.

	experimental	theoretical
NH_2	11.14	10.4
$NHCH_3$	8.80	9.75
$NHCH_2CHCH_2$	-	9.92
$NHCH_2CCH$	-	10.27
$N(CH_3)_2$	8.24	9.38

In summary, this new synthetic route to obtain 8–amino BODIPYs opens the door to the achievement of new efficient and stable blue–emitting laser dyes, where the inherent advantages of the BODIPY dyes are kept, but in the blue spectral region, an almost unexploited region up to now with these kinds of fluorophores. The electron releasing ability of the amine induced the appearance of a hemicyanine–like delocalization which is the responsible of the bright blue emission. The electron donor character of the amine and hence its influence in the photophyscis can be easily controlled by the amine substitution. Although electron donor amines are required for the blue shift, a too larger electron releasing effect is deleterious for the fluorescence capacity due to the formation of a quenching ICT state.

4. Red–Emitting BODIPYs:

Nowadays there is a great research activity focused on the development of competitive red laser dyes owing to the technological advantages and applications of lasers working in this region. Probably, the most important drawback of red laser dyes is their lack of efficiency and stability. This is attributed to proximity of the ground and excited state. Therefore, the goal is to develop laser dyes with improved behaviour. Considering the nice lasing action of BODIPYs in the middle energetic part of the visible, these should be an excellent scaffold to overcome such limitation of red–emitting dyes. The shift of the spectral bands to lower energies is much more easy than to higher energies, because it can be accomplished quite easily just extending the delocalized π–system. Indeed, several strategies have been exploited to this aim. Among them, the most commons are fusing aryl rings to the core, replacing carbons by heteroatoms or attaching aromatic substituents to the chromophore [70–74]. We have chosen the last one and have incorporated *para* substituted phenyl groups at positions 3 and 5 of the chromophore (Scheme 4) [125].

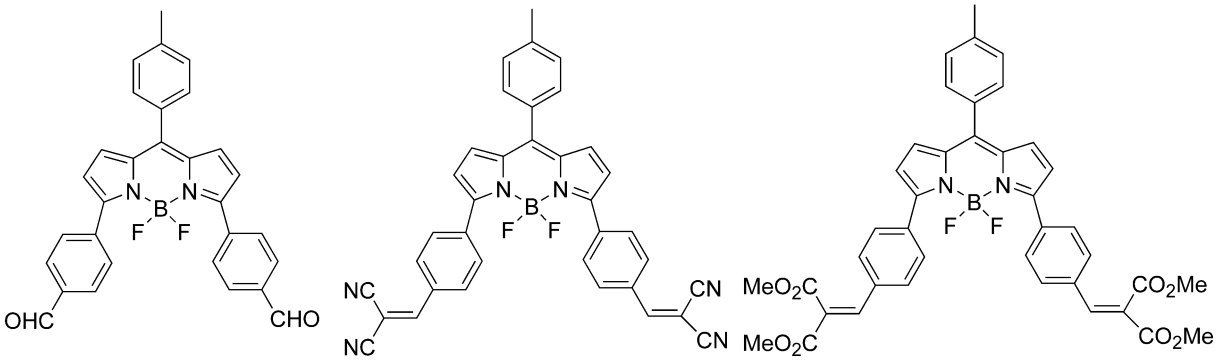

Scheme (4): Molecular structures of the synthesized BODIPYs with red–shifted emission.

The new 3, 5 disubstituted BODIPYs present absorption and fluorescence bands located at around $\lambda_{ab} \approx$ 550-575 nm and $\lambda_{fl} \approx$ 595-625 nm (Figure 11), shifted toward the red spectral region with respect to related alkyl–substituted BODIPY dyes with absorption and fluorescence bands at the green/yellow spectral region. The absorption and fluorescence bands are well separated each other, leading to a large Stokes shift ($\Delta\nu_{St} \approx$ 1200–1800 cm^{-1}), about 3 times higher than that of typical of BODIPY. Fluorescent dyes with large Stokes shifts are of special interest in photonic because the loss of the emission intensity by reabsorption effects at high concentrations, one of the main factors contributing to the losses in the resonator cavity of dye laser, is reduced, and hence it should favour the laser emission efficiency. The new dyes are also characterized by broad spectral bands, mainly for dye **4** (fwhm ≈ 2200 cm^{-1}).

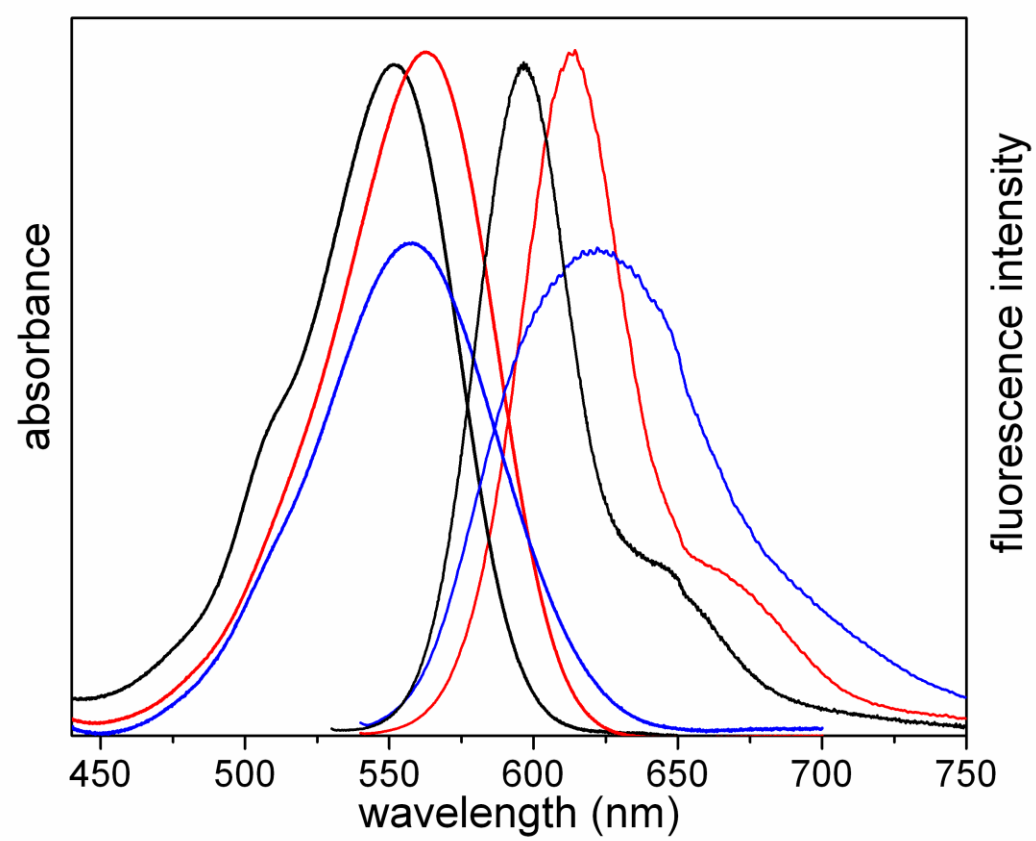

Figure (11): Absorption and fluorescence spectra of red-emitting BODIPYs bearing *para* substituted phenyl groups with aldehide (black), esther (red) and cyano (blue) in trifluoroethanol.

The corresponding HOMO and LUMO molecular orbitals, depicted in Figure 12, show that the electronic π–system is not only localized in the BODIPY core but is extended through the substituents attached at the positions 3 and 5 of the core. This high delocalization in the electronic π–system should be the responsible for the large spectral red shifts observed for these dyes. The optimized geometry in the ground state shows a nearly planar BODIPY core, with the phenyl unit at the *meso* position twisted 51º, and does not take part in the delocalized system, whereas and the aromatic rings at positions 3 and 5 twisted around 30º, and participates in the whole chromophoric π–system. Upon excitation, the electronic distribution (see LUMO map) is extended to the vinyl group at *para* position of the phenyl substituents at positions 3 and 5. Consequently the fluorescence band is more extended red–shifting, explaining the above commented large Stokes shift of these compounds. These red displacements are more prominent for dyes bearing dimethoxycarbonylvnyl or dicyanovinyl

than diformaldehyde (Figure 11), probably because of the presence of vinyl groups in the former dyes and stronger electron withdrawing units at the *para*–phenyl position (methylformate or cyano versus formaldehyde). The inclusion of *p*–substituted-phenyl groups to the core result in more polar BODIPY dyes, as is reflected by the calculated higher values of the dipole moments and their lower solubility in apolar media (i.e. c–hexane).

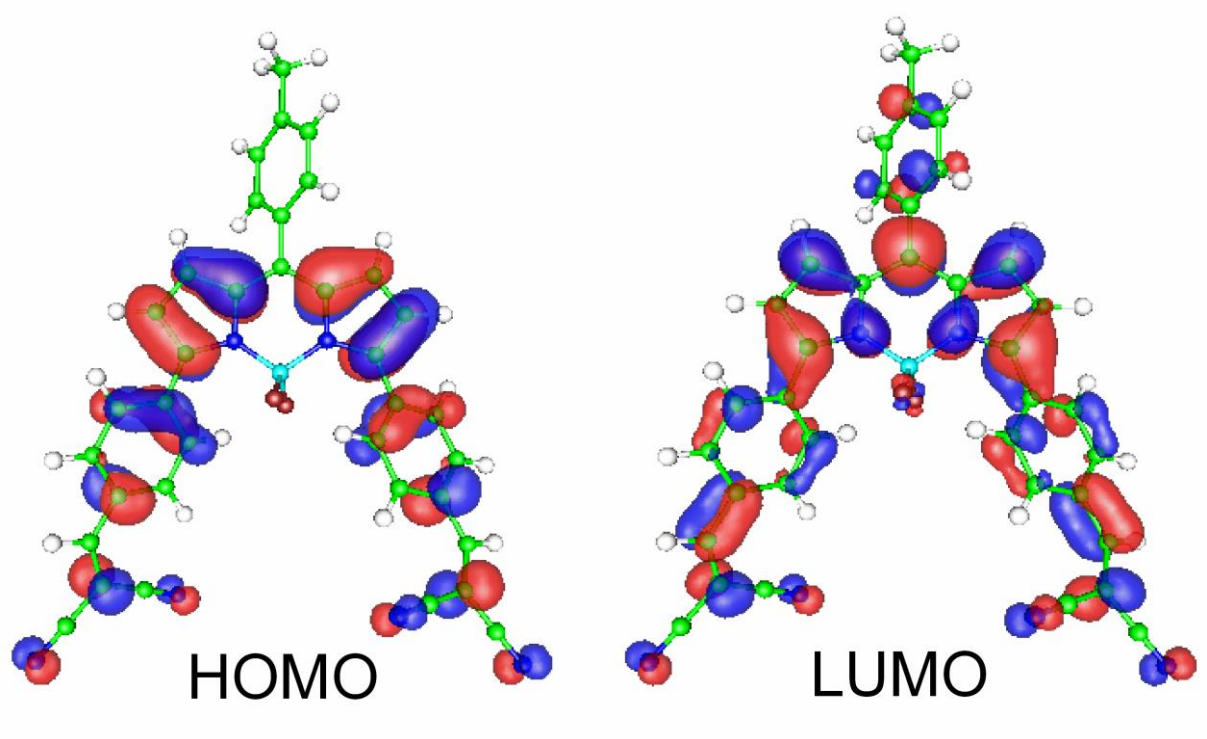

Figure (12): Representative HOMO and LUMO contour maps of one of the red–emitting BODIPYs.

The photophysical parameters of the red BODIPYs in several solvents are summarized in Table 6. The fluorescence quantum yield and lifetime ($\phi \approx 0.40–0.65$, and $\tau \approx 3.5–5.0$ ns, respectively) of these compounds are relatively high, in spite of the red emission of these dyes. In fact, systems with low $S_1–S_0$ energy have low fluorescent capacities because the non–radiative deactivation processes are favoured via a rapid internal conversion mechanism [126,127]. The increase in the internal conversion is probably the most critic issue to develop successfully efficient red emitting dyes. However, present red–emitting BODIPY dyes are characterized by a relative low non–radiative rate constant ($k_{nr} < 1.5\times10^8$ s^{-1}) and a relative high fluorescence rate constant ($k_{fl} \approx 1.3\times10^8$ s^{-1}, despite of the low absorption probability, molar absorption $\varepsilon_{max} \approx 1–3\times10^4$ $M^{-1}cm^{-1}$). Moreover, it has been previously probed that these dyes with a pendant phenyl group at the *meso* 8-position can enhance the internal conversion process via a rotational motion of the phenyl group, reducing the fluorescence efficiency [128,129]. In the present cases, such a mechanism seems to have a minor effect, probably due to the high delocalization of the chromophoric π–system through the aromatic substituents at the opposite positions 3 and 5, which moves further away the electronic density from the central *meso* position.

In general, the compound bearing cyano group, presents the lowest fluorescent efficiency while the rest of the red BODIPYs show the highest ϕ value. The presence of electron withdrawing cyano groups induces a decrease in the k_{fl} value, which is correlated with a lower absorption probability. Although this reduction in the fluorescence ability will reduce the

capacity of this compound to laser, its high Stokes shift would decrease the losses in the resonator cavity favouring its laser action.

Table (6): Photophysical properties of the red–emitting dyes (Scheme 4) in polar (acetone and ethyl acetate) and polar/protic solvents (ethanol, methanol and F_3–ethanol).

	λ_{ab} (nm)	ε_{max} ($10^4 M^{-1}cm^{-1}$)	λ_{fl} (nm)	ϕ	τ (ns)	k_{fl} ($10^8 s^{-1}$)	k_{nr} ($10^8 s^{-1}$)	$\Delta\nu_{St}$ (cm^{-1})
aldehide								
F_3–ethanol	551.5	3.0	595.5	0.58	4.54	1.28	0.92	1365
methanol	557.0	3.1	598.0	0.46	3.65	1.26	1.48	1225
ethanol	559.0	3.1	600.5	0.53	3.91	1.35	1.20	1250
acetone	558.5	3.1	599.5	0.51	3.48	1.46	1.41	1225
ethyl acetate	558.0	3.0	599.0	0.57	3.67	1.55	1.17	1240
esther								
F_3–ethanol	562.5	1.8	613.5	0.59	4.98	1.18	0.82	1470
methanol	570.0	1.9	618.5	0.60	4.56	1.31	0.88	1380
ethanol	573.5	1.9	621.0	0.62	4.67	1.33	0.81	1330
acetone	572.5	1.9	620.0	0.61	4.61	1.32	0.84	1345
ethyl acetate	572.0	1.9	620.0	0.64	4.56	1.40	0.79	1355
cyano								
F_3–ethanol	558.0	0.6	622.0	0.42	4.80	0.87	1.21	1845
methanol	564.0	0.7	623.0	0.41	4.53	0.90	1.30	1675
ethanol	566.0	0.6	625.0	0.47	4.59	1.02	1.15	1665
acetone	565.5	0.6	625.0	0.44	4.80	0.92	1.16	1690
ethyl acetate	563.0	0.6	617.5	0.54	4.66	1.16	0.98	1570

The photophysical behaviour of the new red emitting dyes is compared with other structural related 8–tolyl–BODIPYs found in the literature (Scheme 5) [130,131]. The unsubstituted 8–tolyl–BODIPYs presents a very low fluorescence quantum yield, attributed to an important internal conversion deactivation via the free rotational motion of the pendant 8–aryl group [132,133]. Although, red–emitting dyes usually are characterized by a lower fluorescence capacity because the low S_0–S_1 energy gap favours the internal conversion processes, in terms of the energy gap law [126,127], the incorporation of 3,5–phenyl groups in 8–tolyl–BODIPY not only leads to a large red shift, but also to a progressive enhancement of the fluorescence quantum yield (Scheme 5). Experimental results suggest that the internal conversion of 8–tolyl–BODIPYs is drastically reduced when aryl groups are incorporated at 3 and 5 positions of BODIPY core. The π–electronic delocalization through these groups induces a double bond character to the linking BODIPY-phenyl bonds, reducing the rotational motion of these aryl groups. Moreover, this extended π–system also reduces the electronic density at the *meso* 8–carbon of the BODIPY core, mainly in the excited state (Figure 12), decreasing the effect of the 8-aryl rotation on the internal conversion of these dyes. The substituent effect into the 8–phenyl motion, and hence in the fluorescence ability, will be deeply analyzed in the next section dealing about halogenated BODIPYs. The fluorescence band of the new dyes considered in this work are more extensively red–shifted and with a higher fluorescence quantum yield than structural related derivatives because the presence of adequate

para–substituents at the 3,5-phenyl groups favours the delocalization of the π–system through these moieties increasing their fluorescence ability (Scheme 5).

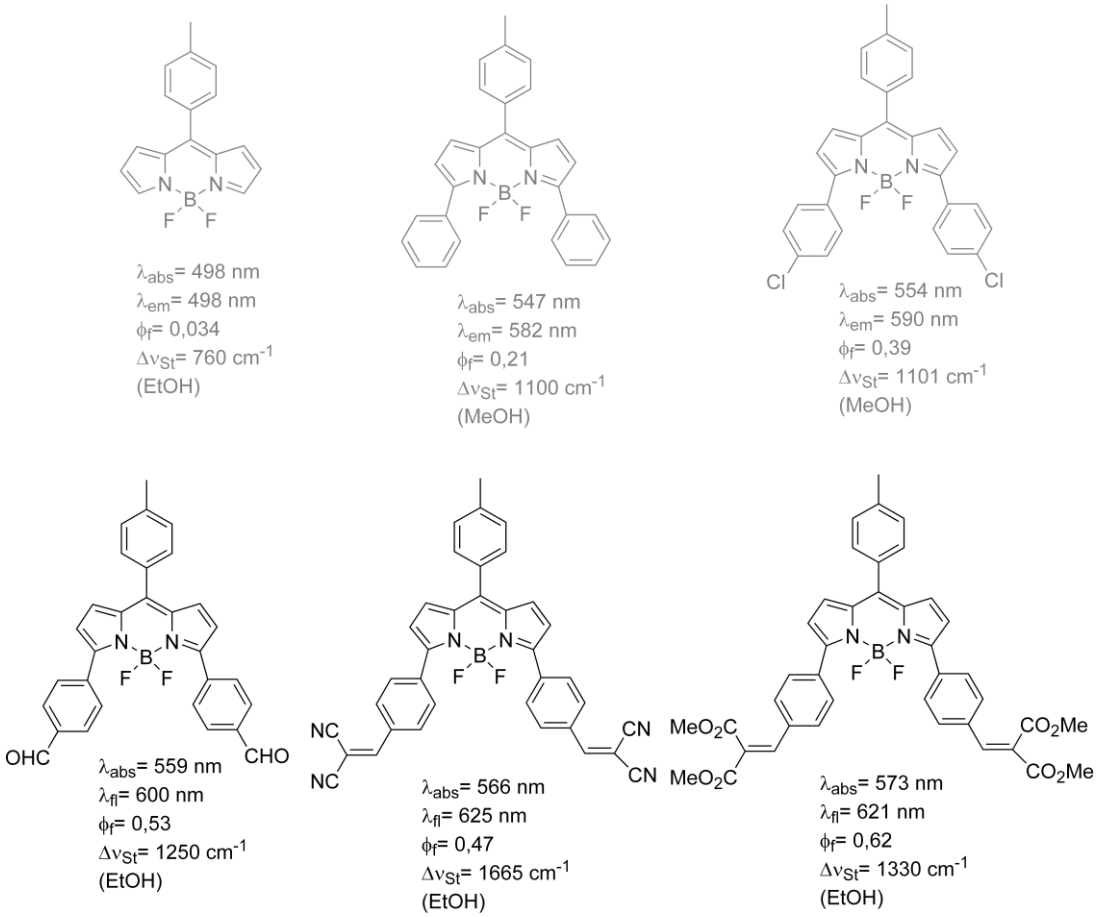

Scheme (5): Comparison of the photophysical behaviour of the 8–tolil–BODIPYs bearing *para* substituted phenyl rings at positions 2 and 5, with structural related derivatives described in the bibliography (grey shaded).

Therefore, present red–emitting BODIPY dyes show an important fluorescence capacity in the red part of the visible region and are promising candidates to be used as active media to develop efficient red–dye laser.

5. Halogenated BODIPYs as Singlet Oxygen Generators Dyes:

Another alternative way to achieve the above commented red shift of the emission band is by attaching halogens to the BODIPY core. Nonetheless, one should expect an important decrease of the fluorescence ability due to the heavy atom effect. Therefore, such halogenated derivatives are not adequate as active media of tunable dye laser. However, the heavy atom effect activates the intersystem crossing pathway, which usually is almost negligible in BODIPYs, and populates the triplet state. Recently, a growing interest is being paid to the use of organic molecules as singlet oxygen generators in photodynamic therapy for the treatment of tumoral cells [134–139]. The idea is to generate singlet oxygen via the triplet state of a sensitizer (organic molecule) upon light irradiation. Considering the chemical stability, versatility and the possibility to modulate the photophysical properties of BODIPY by its functionalization, they are promising candidates as singlet oxygen generators [140–146]. In this section, a battery of iodinated BODIPY derivatives will be thoroughly analyzed (Scheme

6) and the effect of the iodine atom, their number and the position in which they are attached to the BODIPY core will be carefully described [147].

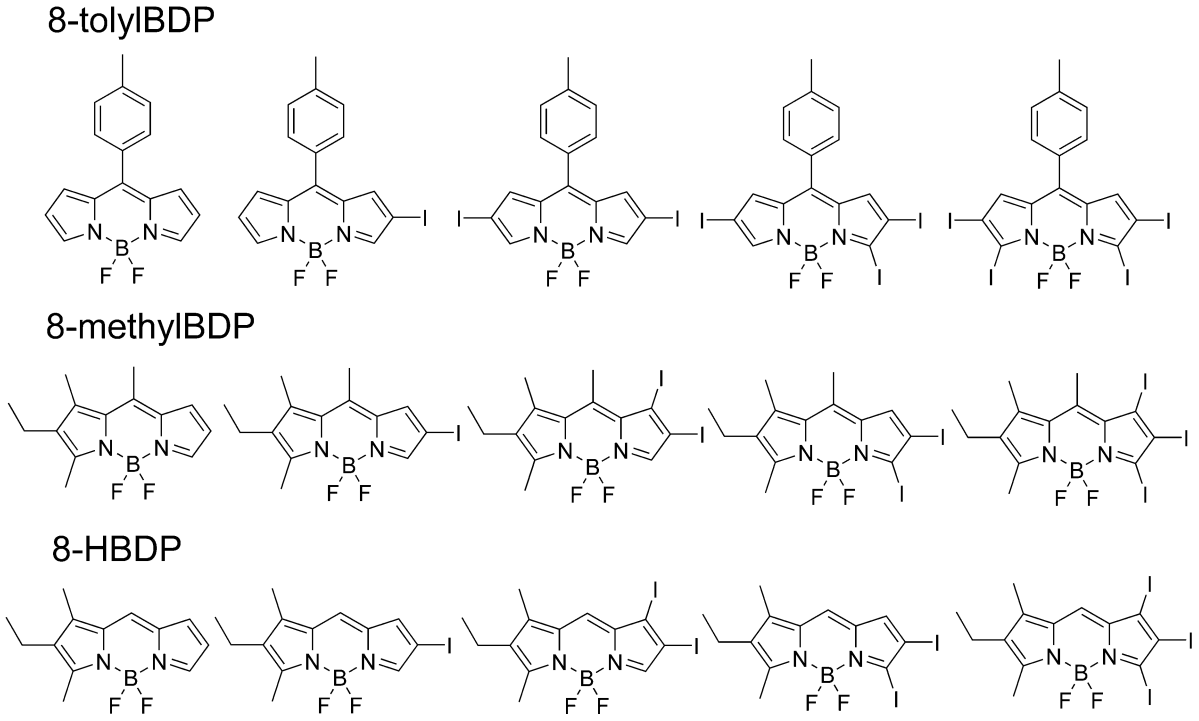

Scheme (6): 8–tolil, 8–methyl and 8–H–BODIPYs and their respective mono, di, tri and tetraiodinated derivatives.

5.1. Iodinated 8-tolil BODIPY derivatives:

The photophysical properties of the 8–tolyl–BODIPY (Table 7) are governed by the presence of the phenyl group at *meso* position. It has been previously claimed the key role of the free motion of such ring, which greatly increases the internal conversion processes. Furthermore, a possible interaction of the aryl with the BODIPY distorting the indacene planarity has been also reported [148–150]. The absence of substituents at positions 1 and 7 enables the rotation of the phenyl ring (twisted 50º) [151, 152]. Hence, this dye is characterized by a very low fluorescence quantum yield ($\phi < 0.04$) and lifetime ($\tau < 700$ ps). Indeed, the hampering of the free motion of the phenyl or its blockade in a perpendicular disposition, due to the sterical hindrance forced by substitution at the chromophoric adjacent positions to the *meso* as well as by attaching bulky groups to the *orto* positions of the phenyl, led to a recovering all the typical high fluorescence capacity of the BODIPY [9].

Owing to the electronegativity of the iodine atom the incorporation of such halogen to BODIPY should take place via an electrophilic substitution. Thus, those chromophoric positions with the highest negative charge should be more susceptible to be iodinated, except positions 1 and 7, where the sterical hindrance between the phenyl ring and the bulk iodine atom avoids the halogenation of such positions. The theoretically predicted electronic charge distribution nicely indicates the position to be first iodinated (Figure 13) and the following positions to suffer the electrophylic attack, after the consequence charge rearrangement, in good agreement with the experimental findings.

Table (7): Photophysical properties of all the iodinated BODIPYs (Scheme 6) in a common solvent (cyclohexane)

	l_{ab} (nm)	e_{max} ($10^4 M^{-1}cm^{-1}$)	l_{fl} (nm)	f	t (ps)
8-tolil-BODIPYs					
8-tolilBDP	500.5	6.9	516.0	0.036	323
monoI	523.5	2.2	540.0	0.034	184
diI	548.5	4.3	567.5	0.012	117
triI	563.5	4.8	577.5	0.060	327
tetraI	581.0	11.6	593.0	0.099	678
8-methyl-BODIPYs					
8-methylBDP	504.0	3.3	515.0	0.96	5460
monoI	517.5	4.6	532.0	0.13	560
diI(6,7)	515.5	2.9	538.5	0.05	259
diI(5,6)	532.0	9.8	546.0	0.20	1021
triI	531.5	1.7	554.5	0.10	331
8-H-BODIPYs					
8-HBDP	512.5	2.9	517.5	0.70	5240
monoI	528.0	6.3	538.5	0.11	489
diI(6,7)	527.5	5.6	537.0	0.05	212
diI(5,6)	542.0	7.6	550.5	0.26	1041
triI	543.5	6.9	551.5	0.07	358

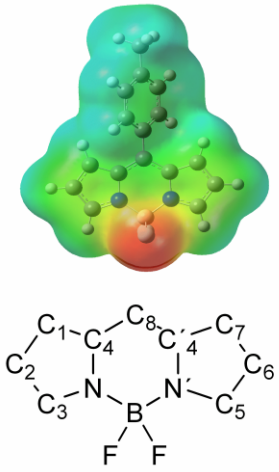

	8-tolil	mono-I	di-I	tri-I	tetra-I
C1	-0,337	-0,258	-0,255	-0,255	-0,25
C2	-0,291	-0,347	-0,35	-0,349	-0,249
C3	-0,143	-0,093	-0,089	-0,087	-0,265
C4	0,251	0,247	0,246	0,254	0,224
C´4	0,251	0,253	0,249	0,219	0,224
C5	-0,143	-0,139	-0,089	-0,265	-0,265
C6	-0,291	-0,289	-0,35	-0,251	-0,249
C7	-0,337	-0,334	-0,255	-0,259	-0,25
C8	0,174	0,173	0,172	0,174	0,175
N	-0,217	-0,214	-0,215	-0,218	-0,194
N´	-0,217	-0,217	-0,215	-0,191	-0,194

Figure (13): Ground state charge distribution of 8–tolil–BODIPY and its halogenated (up to four iodine atoms). The electrostatic potential mapped onto the electronic density for the reference compound is also included.

The iodination of the BODIPY gives rise to bathochromic shift of the spectral bands, which is much larger increasing the number of the attached iodines (Figure 14). In fact, the tetraiodinated derivative emits in the red part of the visible (around 590 nm). As was expected, the halogenation of the BODIPY core induces a further decrease in the fluorescence capacity owing to the heavy atom effect, which increases the intersystem crossing probability (Table 7). However, such trend holds true for the first and second iodination at positions 2 and

6. Surprisingly, further addition of iodine to the BODIPY core leads to a recovery of both the absorption and fluorescence capacity. For instance, the tetraiodinated derivative shows a very high molar absorption (around 11×10^4 M^{-1} cm^{-1}, twice the non–iodinated BODIPY) and even higher than typical BODIPYs **(**9×10^4 M^{-1} cm^{-1}) [9], in spite of the halogens presence. Besides, the fluorescence quantum yield enhances up to 0.1, improving the fluorescence ability of the reference non–iodinated BODIPY**.** Such dye shows a uniform charge distribution in the pyrrole, whereas in the rest of the 8–tolil iodinated BODIPY derivatives it was more heterogeneous. That means that the negative charge in the nitrogen and carbons at positions 1, 2 and 3, and their corresponding symmetrical ones, is nearly the same (around –0.255). Accordingly, the delocalization is improved, in concordance with the push-pull effect (substitution at the beginning and ending of the delocalized system) [131]. Therefore, substitution at positions 3 and 5 counteracts in part the non-radiative processes (heavy atom effect and phenyl free motion) ameliorating the fluorescence efficiency of the dye. It seems that the iodine presence at those positions extents the chromophoric electronic density far away from the phenyl ring diminishing the deleterious effect in fluorescence owing to its free motion, in agreement with the experimental findings obtained for the red–emitting BODIPYs discussed in the preceding section.

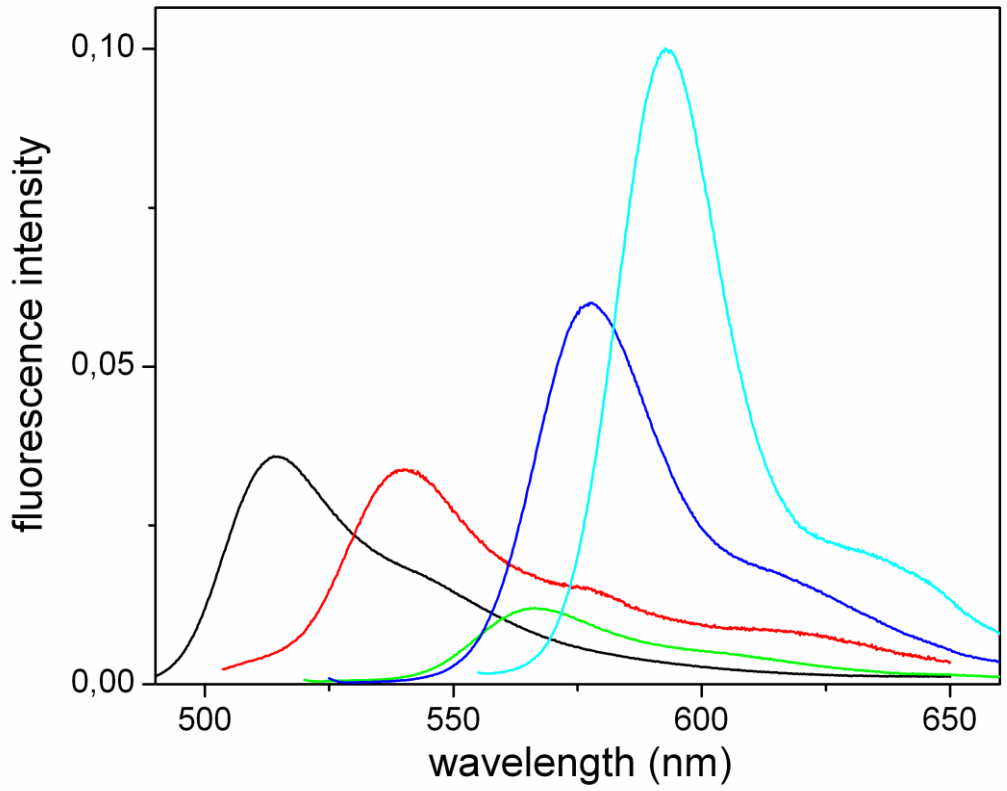

Figure (14): Fluorescence spectra of 8–tolyl–BODIPY and its halogenated derivatives with one (black), two (red), three (blue) and four (cyano) iodine atoms.

As main conclusion, the halogenation favour the triplet state population in detriment of the fluorescence capacity, but the magnitude of such effect clearly depends on the position in which the iodine is attached. This is due to the presence of the phenyl group with free motion at meso position, and the dependency of its deleterious influence in fluorescence with regard to the electronic density around the central BODIPY position.

5.2. Iodinated 8-methyl- and 8-H-BODIPY derivatives:

Apart of the above commented BODIPYs bearing tolyl unit, iodine has been incorporated also in BODIPYs with one pyrrole fully alkylated. Two set of derivatives were considered those derived from a BODIPY with methyl group at its *meso* position and without it. Surprisingly, although in one of the reference compound the *meso* position is free and characterized by a high negative charge, therefore ready to an electrophilic substitution by iodine, such position could not be iodinated. Figure 15 indicates that the dipole moment of the BODIPY is oriented through the transversal axis with the negative charge mainly placed around the BF_2 linking bridge, whereas the positive charge located around the central position. Probably, although the carbon at position 8 has a net negative charge the surrounding positive charge avoids the approach of the iodine, and preventing the halogenation of such position

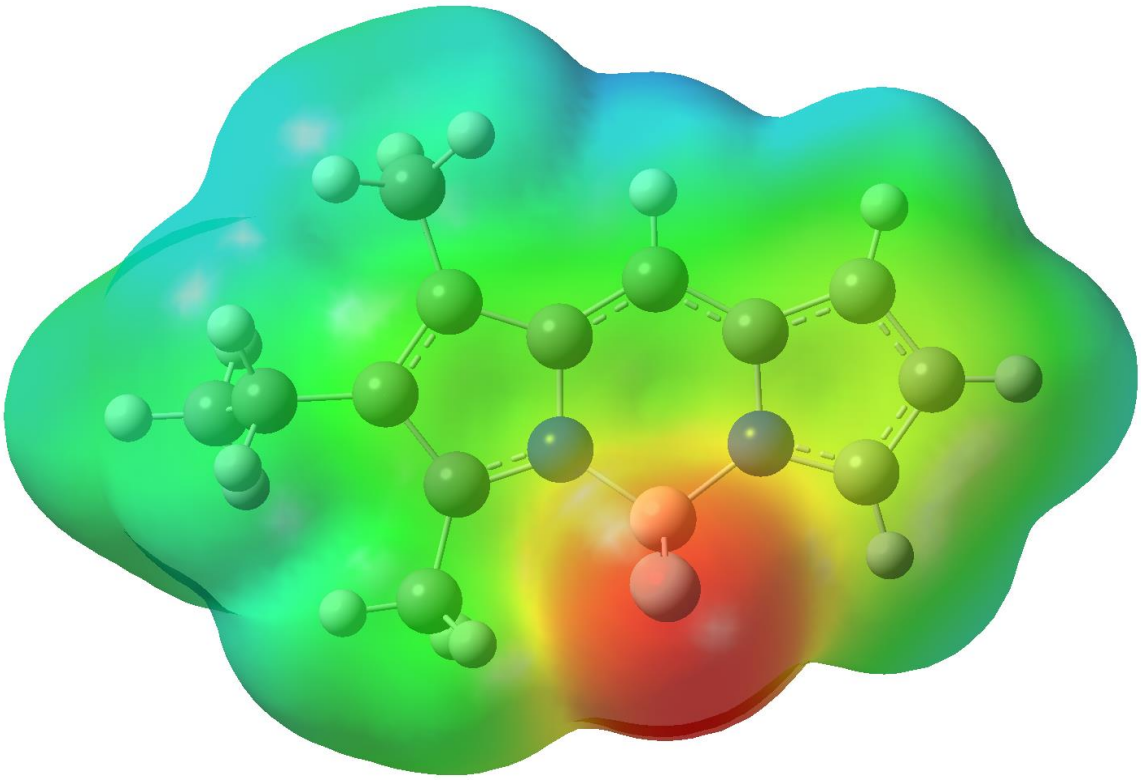

Figure (15): Electrostatic potential mapped onto the electronic density (negative in red color and positive in blue color) of the 8–H–BODIPY.

The absence of the bulky and mobile phenyl group in the reference non-halogenated compounds leads to highly fluorescence dyes, as expected for alkyl–BODIPYs (Table 7). The absorption probability is not very high due to the asymmetric substitution pattern which leads to charge separation between the pyrroles. The incorporation of an iodine atom at position 6 implies a drastic decrease of the fluorescence ability, which is attributed to the enhancement in the probability of intersystem crossing, as describe above (Table 7). Nonetheless, further halogenation leads to entirely different results depending of the position in which the iodine is attached. The iodination at position 7 hardly affects the spectral band position and induces a further reduction of the fluorescence ability, in agreement with an additive heavy atom effect. In contrast, the iodination at position 5 gives rise to a bathochromic spectral shift as well as an improvement in both the absorption probability and fluorescence efficiency (Table 7), in concordance with the push-pull effect. Again, this

enhancement in fluorescence coincides with an uniform electronic distribution in the pyrrole rings, in concordance with the trends obtained in the 8–tolyl–BODIPY. Therefore, present results confirm that substitution and the extremes of the delocalized π–system is advantageous for the fluorescence ability of the dye. In the triiodinated derivatives, the presence of iodine at positions 5 and 7 has contrary influence in the photophysics of the dye. As result, the effect of both iodine atoms is counteracted. That means, whereas substitution at position 7 should increase the intersystem crossing, without altering the band position, substitution at position 5 should favour the fluorescence ability and give rise to a bathochromic shift. Consequently, their spectral bands are placed close to those of the diiodinated derivative at positions 5 and 6, whereas their fluorescence capacity is similar to that of the monoiodinated ones (Table 7). Indeed, the electronic distribution in the triiodinated derivatives is less uniform and the system is less aromatic.

Finally, we should note the close correlation between the fluorescence quantum yield and the lifetime with both changing the number of halogens appended to BODIPY and the environmental properties (Table 7). Such evolutions are controlled mainly by the non–radiative processes, thus the lower the fluorescence efficiency the faster the decay from the excited state.

Summing up, upon iodination of the BODIPYs we have converted a fluorescence dye characterized by a nearly negligible intersystem crossing probability into a promising singlet oxygen sensitizer populating the triplet state making use of the so–called internal heavy atom effect. Afterwards the energy transfer from excited triplet state to dissolved ground state oxygen should lead to the singlet oxygen generation. Indeed, preliminary transient absorption measurements confirm the triplet state populations and single oxygen generation for iodinated BODIPYs with quantum yields in the range of compounds recognized as efficient singlet oxygen photosensitizer (Rose Bengal), suggesting that they could work as photodynamic therapy agents.

6. Conclusions:

The high and increasing number of publications on BODIPY indicates they are becoming some of the most used dyes not only for laser production, but also for a wide variety of technological applications including biomedicine. Their success may be, in part, due to their stability and versatility. Almost all the available positions of BODIPY can be functionalized with the desired entity. Furthermore, the substitution pattern of the core and the position where the groups are attached will determine the photophysical properties of the resulting BODIPY. In other words, tailor-made BODIPY can be designed for almost any wanted application.

Here, we have made use of such advantages to span the BODIPY work region to the blue as well as to the red part of the visible spectrum. Therefore, the whole visible region can be covered with the same dye family and an efficient and stable laser signal can be achieved in the desired wavelength. A red shift can be easily achieved by increasing the delocalization through adequate aromatic substituents. Thus, BODIPY efficiently emitting into the red can be obtained. On the other hand, the emission may also be shifted deep into the blue by the incorporation of amino groups at their *meso* position. The electron releasing effect of the amine induces the appearance of a hemicyanine–like resonant structure responsible for the bright blue emission. Controlling the electron donor character of the amine by its substitution allows the modulation of the spectral bands positions.

A clear proof of the versatility of BODIPY fluorophores is their use as singlet oxygen photosensitizers in photodynamic therapy. At first sight, these molecules are not adequate because BODIPY are notable for their low intersystem crossing probability and the triplet state population is a key feature for singlet oxygen generators. However, the halogenation of BODIPY (up to four iodine atoms can be directly attached to the core) transforms a highly fluorescence dye in a molecule with a high triplet state population. Thus, these iodinated BODIPY should work as singlet oxygen photosensitizer in photodynamic therapy.

7. Acknowledgements:

E. Peña (Universidad de Guanajuato, Mejico) and M. J. Ortiz (Universidad Complutense, Madrid), A. Costela and I. Garcia Moreno (CSIC, Madrid) are thanked for their collaboration in the synthesis of new BODIPY dyes and the lasing characterization, respectively. Gobierno Vasco (IT339−10) and Spanish MICINN (MAT2010-20646-C04-04) are gratefully thanked by financial support.

8. References:

[1] M. Maeda, Laser Dyes. (Academic Press, Tokyo, 1984).
[2] F. P. Schäfer, Dye Lasers. (3rd Ed., Springer−Verlag, Berlin, 1990).
[3] A. Prasanna de Silva, H. Q. N. Gunaratne, T. Gunnlaugsson, A. J. M. Huxley, C. P. McCoy, J. T. Rademacher, and T. E. Rice, Chem. Rev. 97 (1997) 1515.
[4] B. Valeur, and I. Leray, Coord. Chem. Rev. 205 (2000) 3.
[5] K. Rurack, and U. Resch−Genger, Chem. Soc. Rev. 31 (2002) 116.
[6] H. Zollinger, Color Chemistry (3rd Ed.,Wiley-VCH, Zurich, 2003).
[7] J. R. Lakowicz, Principles of Fluorescence Spectroscopy (3rd Ed., Springer, Singapore, 2006).
[8] A. Costela, I. García−Moreno, R. Sastre, Phys. Chem. Chem. Phys. 5 (2003) 4745.
[9] F. López Arbeloa, J. Bañuelos, V. Martínez, T. Arbeloa, and I. López Arbeloa, Int. Rev. Phys. Chem. 24 (2005) 339.
[10] A. Loudet, K. Burgess, Chem. Rev. 107 (2007) 4891.
[11] T. E. Wood, A. Thompson, Chem. Rev. 107 (2007) 1831.
[12] G. Ulrich, R. Ziessel, A. Harriman, Angew. Chem. Int. Ed. 47 (2008) 1184.
[13] M. Benstead, G. H. Mehl, R. W. Boyle, Tetrahedron, 67 (2011) 3573.
[14] A. Treibs, and F. H. Kruzer, Justus Liebigs Ann. Chem. 718 (1968) 208.
[15] T. G. Pavlopoulos, M. Shah, and J. H. Boyer, Appl. Opt. 27 (1988) 4998.
[16] M. Shah, K. Thangaraj, M−L. Soong, L. T. Wolford, J. H. Boyer, I. R. Politzer, and T. G. Pavlopoulos, Heteroat. Chem. 1 (1990) 389.
[17] T. G. Pavlopoulos, J. H. Boyer, M. Shah, K. Thangaraj, and M−L. Soong, Appl. Opt. 29 (1990) 3885.
[18] J. H. Boyer, A. M. Haag, G. Sathyamoorthi, M-L. Soong, K. Thangaraj, and T. G. Pavlopoulos, Heteroat. Chem. 4 (1993) 39.
[19] M. L. Metzker, J. Lu, and R. A. Gibbs, Science 271 (1996) 1420.
[20] S. A. Farber, M. Pack, S−Y. Ho, I. D. Johnson, D. S. Wagner, R. Dosch, M. C. Mullins, H. S. Hendrickson, E. K. Hendrickson, and M E. Halpern, Science 292 (2001) 1385.
[21] R. Reents, M. Wagner, J. Kulhmann, and H. Waldmann, Angew. Chem. Int. Ed. 43 (2004) 2711.
[22] Q. Zheng, G. Xu, P. N. Prasad, Chem. Eur. J. 14 (2008) 5812.
[23] J. Karolin, L. B−A. Johansson, L. Strandberg, and T. Ny, J. Am. Chem. Soc. 116 (1994) 7801.

[24] R. Y. Lai, and A. J. Bard, J. Phys. Chem. B 107 (2003) 5036.
[25] Z. Shen, H. Röhr, K. Rurack, H. Uno, M. Spieles, B. Schulz, G. Reck, and N. Ono, Chem. Eur. J. 10 (2004) 4853.
[26] W. Qin, M. Baruah, M. Van der Auweraer, F. C. De Schryver, and N. Boens, J. Phys. Chem. A 109 (2005) 7371.
[27] A. D. Quartorolo, N. Russo, and E. Sicilia, Chem. Eur. J. 12 (2006) 6797.
[28] S. Badré, V. Monnier, R. Méallet-Renault, C. Dumas–Verdes, E. Y. Schmidt, B. A. Trofimov, and R. B. Pansu, J. Photochem. Photobiol. A 183 (2006) 238.
[29] A. Cui, X. Peng, J. Fan, X. Chen, Y. Wu, and B. Guo, J. Photochem. Photobiol. A 186 (2007) 85.
[30] Y-W. Wang, A. B. Descalzo, Z. Shen, X-Z. You, K. Rurack, Chem. Eur. J. 16 (2010) 2887.
[31] J. Bañuelos, A. R. Agarrabeitia, I. García–Moreno, I. López Arbeloa, A. Costela, L. Infantes, M. E. Pérez–Ojeda, M. Palacios–Cuesta, M. J. Ortiz, Chem. Eur. J. 16 (2010) 14094.
[32] Y. Assor, Z. Burshtein, and S. Rosenwaks, Appl. Opt. 37 (1998) 4914.
[33] M. S. Mackey, and W. N. Sisk, Dyes and Pigments 51 (2001) 79.
[34] G. Jones II, O. Klueva, S. Kumar, and D. Pacheco, Int. Soc. Opt. Eng. 4267 (2001) 24.
[35] M. D. Rahn and T. A. King, Appl. Opt. 34 (1995) 8260.
[36] E. Yariv, S. Schultheiss, T. Saraidarov, and R. Reisfeld, Opt. Mater. 16 (2001) 29.
[37] A. Costela, I. García-Moreno, and R. Sastre, in Handbook of Advanced Electronic and Photonic Materials and Devices, Edited by H. S. Nalwa (Academic Press, San Diego, 2001).
[38] M. Ahmad, T. A. King, D–K. Ko, B. H. Cha, and J. Lee, J. Phys. D 35 (2002) 1473.
[39] A. Costela, I. García–Moreno, and R. Sastre, Phys. Chem. Chem. Phys. 5 (2003) 4745.
[40] R. K. Lammi, A. Ambroise, T. Balasubramanian, R. W. Wagner, D. F. Bocian, D. Holten, and J. S. Lindsey, J. Am. Chem. Soc. 122 (2000) 7579.
[41] H. Imahori, H. Norieda, H. Yamada, Y. Nishimura, I. Yamazaki, Y. Sakata, and S. Fukuzumi, J. Am. Chem. Soc. 123 (2001) 100.
[42] A. Ambroise, C. Kirmaier, R. W. Wagner, R. S. Loewe, D. F. Bocian, D. Holten, and J. S. Lindsey, J. Org. Chem. 67 (2002) 3811.
[43] S. Hattori, K. Ohkubo, Y. Urano, H. Sunhara, T. Pagano, Y. Wada, N. V. Tkachenko, H. Lemmetyinen, and S. Fukuzumi, J. Phys. Chem. B 109 (2005) 15368.
[44] F. D´Souza, P. M. Smith, M. E. Zandler, A. L. McCarty, M. Itou, Y. Araki, O. Ito, J. Am. Chem. Soc. 126 (2004) 7898.
[45] L. Wu, A. Loudet, R. Barhoumi, R. C. Burghardt, K. Burgess, J. Am. Chem. Soc. 131 (2009) 9156.
[46] R. Ziessel, G. Ulrich, K. J. Elliott, A. Harriman, Chem. Eur. J. 15 (2009) 4980.
[47] O. A. Bozdemir, Y. Cakmak, F. Sozmen, T. Ozdemir, A. Siemiarczuk, E. U. Akkaya, Chem. Eur. J. 16 (2010) 6346.
[48] R. Ziessel, A. Harriman, Chem. Commun. 47 (2011) 611.
[49] S. Blaya, P. Acebal, L. Carretero, and A. Fimia, Opt. Comun. 228 (2003) 55.
[50] S. Y. Lam, and M. J. Damzen, Opt. Commun. 218 (2003) 365.
[51] R. Jakubiak, L. V. Natarajan, V. Tondiglia, G. S. He, P. N. Prasad, T. J. Bunning, and R. A. Vaia, Appl. Phys. Lett. 85 (2004) 6095.
[52] M. Baruah, W. Qin, N. Basaric, W. M. De Borggraeve, and N. Boens, J. Org. Chem. 70 (2005) 4152.
[53] M. Baruah, W. Qin, C. Flors, J. Hofkens, R. A. L. Vallée, D. Beljonne, M. Van der Auweraer, W. M. De Borggraeve, and N. Boens, J. Phys. Chem. A 110 (2006) 5998.
[54] H. Sunahara, Y. Urano, H. Kojima, and T. Pagano, J. Am. Chem. Soc. 129 (2007) 5597.

[55] Y. Ando, S. Iino, J. Yamada, K. Umezawa, N. Iwasawa, D. Citterio, and K. Suzuki, Sensors and Actuators B 121 (2007) 74.
[56] O. A. Bozdemir, R. Guliyev, O. Buyukcakir, S. Selcuk, S. Kolemen, G. Gulseren, T. Nalbantoglu, H. Boyaci, E. U. Akkaya, J. Am. Chem. Soc. 132 (2010) 8029.
[57] K. Rurack, M. Kollmannsberger, U. Resch–Genger, and J. Daub, J. Am. Chem. Soc. 122 (2000) 968.
[58] C. Goze, G. Ulrich, L. Charbonnière, M. Cesario, T. Prangé, and R. Ziessel, Chem. Eur. J. 9 (2003) 3748.
[59] Y. Gabe, Y. Urano, K. Kikuchi, H. Kojima, and T. Nagano, J. Am. Chem. Soc. 126 (2004) 3357.
[60] H. Koutaka, J. Kosuge, N. Fukasaku, T. Hirano, K. Kikuchi, Y. Urano, H. Kojima, and T. Nagano, Chem. Pharm. Bull. 52 (2004) 700.
[61] J. L. Bricks, A. Kovalchuk, C. Trieflinger, M. Nofz, M. Büschel, A. I. Tomalchev, J. Daub, and K. Rurack, J. Am. Chem. Soc. 127 (2005) 13522.
[62] K. Yamada, Y. Nomura, D. Citterio, N. Iwasawa, and K. Suzuki, J. Am. Chem. Soc. 127 (2005) 6956.
[63] N. Basaric, M. Baruah, W. Qin, B. Metten, M. Smet, W. Dehaen, and N. Boens, Org. Biomol. Chem. 3 (2005) 2755.
[64] H. Lu, S. Zhang, H. Liu, Y. Wang, Z. Shen, C. Liu, X. You, J. Phys. Chem. A 113 (2009) 14081
[65] C. Garzillo, R. Improta, and A. Peluso, J. Molec. Struct. 426 (1998) 145.
[66] W. M. F. Fabian, and J. M. Kauffman, J. Lumin 85 (1999) 137.
[67] W. M. F: Fabian, K. S. Niederreiter, G. Uray, and W. Stadlbauer, J. Molec. Struct. 477 (1999) 209.
[68] J–R. Hill, L. Subramanian, and A. Maiti, Molecular Modeling Techniques in Materials Science (Taylor & Francis, Boca Raton, 2005).
[69] H–D. Höltje, W. Sippl, D. Rognan, and G. Folkers, Molecular Modeling (Wiley–VCH, Weinheim, 2008)
[70] W. Zhao, E. M. Carreira, Chem. Eur. J. 12 (2006) 7254.
[71] K. Umezawa, Y. Nakamura, H. Makino, D. Citterio, K. Suzuki, J. Am. Chem. Soc. 130 (2008) 1550.
[72] K. Umezawa, A. Matsui, Y. Nakamura, D. Citterio, K. Suzuki, Chem. Eur. J. 15 (2009) 1096.
[73] A. B. Descalzo, H–J. Xu, Z-L. Xue, K. Hoffmann, Z. Shen, M. G. Weller, X-Z. You, K. Rurack, Org. Lett. (2011) 1138.
[74] A. Costela, I. García–Moreno, M. Pintado-Sierra, F. Amat–Guerri, M. Liras, R. Sastre, F. López Arbeloa, J. Bañuelos, I. López Arbeloa, J. Photochem. Photobiol. A 198 (2008) 192.
[75] G. Sathyamoorthi, M–L. Soong, T. W. Ross, J. H. Boyer, Heteroatom. Chem. 4 (1993) 603.
[76] T. W. Roos, G. Sathyamoorthi, J. H. Boyer, Heteroatom Chem. 4 (1993) 609.
[77] J. Bañuelos, F. López Arbeloa, V. Martínez, M. Liras, A. Costela, I. García Moreno, I. López Arbeloa, Phys. Chem. Chem. Phys. 13 (2011) 3437.
[78] A. Gorman, J. Killoran, C. O'Shea, T. Kenna, W. M. Gallagher, D. F. O'Shea, J. Am. Chem. Soc., 126 (2004) 10619.
[79] S. Ozlem, E. U. Akkaya, J. Am. Chem. Soc. 131 (2009) 48.
[80] S. H. Lim, C. Thivierge, P. Nowak-Sliwinska, J. Han, H. van den Bergh, G. Wagnières, K. Burgess, H. B. Lee, J. Med. Chem. 53 (2010) 2865.
[81] H. He, P–C. Lo, S–L. Yeung, W–P. Fong, D. K. P. Ng, Chem. Commun. 47 (2011) 4748.

[82] F. López Arbeloa, T. López Arbeloa, I. López Arbeloa, I. García–Moreno, A. Costela, R. Sastre, and F. Amat–Guerri, Chem. Phys. 236 (1998) 331.
[83] J. Bañuelos, F. López Arbeloa, V. Martínez, and I. López Arbeloa, Chem. Phys. 296 (2004) 13.
[84] F. López Arbeloa, T. López Arbeloa, and I. López Arbeloa, in Handbook of Advanced Electronic and Photonic Materials and Devices, Edited by H. S. Nalwa (Academic Press, San Diego, 2001).
[85] T . G. Pavlopoulos, Prog. Quantum Elect. 26 (2002) 193.
[86] Y–H. Yu, Z. Shen, H–Y. Xu, Y–W. Wang, T. Okujima, N. Ono, Y–Z. Li, and X–Z. You, J. Molec. Struct. 827 (2007) 130.
[87] J. Bañuelos, F. López Arbeloa, V. Martínez, T. Arbeloa López, F. Amat–Guerri, M Liras, and I. López Arbeloa, Chem. Phys. Lett. 385 (2004) 29.
[88] F. López Arbeloa T. López Arbeloa, and I. López Arbeloa, J. Photochem. Photobiol. A 121 (1999) 177.
[89] J. Bañuelos, F. López Arbeloa, V. Martínez. T. Arbeloa López, and I. López Arbeloa, J. Phys. Chem. A 108 (2004) 5503.
[90] J. Bañuelos, F. López Arbeloa, V. Martínez, T. Arbeloa López, and I. López Arbeloa, Phys. Chem. Chem. Phys. 6 (2004) 4247.
[91] J. Fabian, and H. Hartmann, Light Absorption of Organic Colorants (Springer–Verlag, Berlin, 1980).
[92] N. Tyultyulkov, J. Fabian, A. Mehlhorn, F. Dietz, and A. Tadjer, Polymethine Dyes (Jusautor, Sofia, 1991).
[93] Y. Marcus, Chem. Soc. Rev. 22 (1993) 409.
[94] A. R. Katritzky, D. C. Fara, H. Yang, K. Tämm, T. Tamm and M. Karelson, Chem. Rev. 104 (2004) 175.
[95] J. Catalan, J. Phys. Chem. B 113 (2009) 5951.
[96] M. J. Kamlet, and R. W. Taft, J. Am. Chem. Soc. 98 (1976) 377.
[97] M. J. Kamlet, and R. W. Taft, J. Am. Chem. Soc. 98 (1976) 2886.
[98] M. J. Kamlet, J. L. M. Abboud, and R. W. Taft, J. Am. Chem. Soc. 99 (1977) 6027.
[99] C. Reichardt, Chem. Rev. 94 (1994) 2319.
[100] F. López Arbeloa, T. López Arbeloa, and I. López Arbeloa, Trends Photochem. Photobiol. 3 (1994) 145.
[101] A. Costela, I. García–Moreno, J. M. Figuera, F. Amat–Guerri, and R. Sastre, Laser Chem. 18 (1998) 63.
[102] F. López Arbeloa, J. Bañuelos, I. López Arbeloa, A. Costela, I. García–Moreno, C. Gómez, F. Amat–Guerri, M. Liras, and R. Sastre, Photochem. Photobiol. 78 (2003) 30.
[103] I. García–Moreno, A. Costela, L. Campo, R. Sastre, F. Amat–Guerri, M. Liras, F. López Arbeloa, J. Bañuelos, and I. López Arbeloa, J. Phys. Chem. A 108 (2004) 3315.
[104] J. Bañuelos, F. López Arbeloa, O. García, and I. López Arbeloa, J. Lumin. 126 (2007) 833.
[105] I. García–Moreno, F. Amat–Guerri, M. Liras, A. Costela, L. Infantes, R. Sastre, F. López Arbeloa, J. Bañuelos, and I. López Arbeloa, Adv. Funct. Mater. 17 (2007) 3088.
[106] O. García, R. Sastre, D. del Agua, A. Costela, I. García–Moreno, F. López Arbeloa, J. Bañuelos, and I. López Arbeloa, J. Phys. Chem. C 111 (2007) 1508.
[107] A. Costela, I. García–Moreno, C. Gómez, O. García, and R. Sastre, J. Appl. Phys. 90 (2001) 3159.
[108] A. Costela, I. García–Moreno, C. Gómez, R. Sastre, F. Amat-Guerri, M. Liras, F. López Arbeloa, J. Bañuelos, and I. López Arbeloa, J. Phys. Chem. A 106 (2002) 7736.
[109] M–S. Schiedel, C. A. Briehn, P. Bäuerle, Angew. Chem. Int. Ed. 40 (2001**)** 4677.
[110] R. Mondal, B. K. Shah, D. C. Neckers, J. Org. Chem. 71 (2006**)** 4085.

[111] A. Pron, G. Zhou, H. Norouzi−Arasi, M. Baumgarten, Org. Lett. 11 (2009**)** 3550.
[112] S−W. Wen, M−T. Lee, C. H. Chen, J. Disp. Tech. 1 (2005) 90.
[113] Z−S. Wang, Y. Cui, K. Hara, Y. Dan−oh, C. Kasada, A. Shinpo, Adv. Mater. 19 (2007) 1138.
[114] X. Zhan, S. Barlow, S. R. Marder, Chem. Comm. 15 (2009) 1948.
[115] Y. Matano, H. Imahori, Org. Biomol. Chem. 7 (2009) 1258.
[116] C. F. A. Gómez−Duran, I. García−Moreno, A. Costela, V. Martin, R. Sastre, J. Bañuelos, F. López Arbeloa, I. López Arbeloa, E. Peña−Cabrera, Chem. Commun. 46 (2010) 5103.
[117] J. Bañuelos, V. Martin, C. F. A. Gómez−Duran, I. J. Arroyo Córdoba, E. Peña−Cabrera, I. García−Moreno, A. Costela, M. E. Pérez−Ojeda, T. Arbeloa, I. López Arbeloa, Chem. Eur. J. 17 (2011) 7261.
[118] C. Hansch, A. Leo, R. W. Taft, Chem. Rev. 91 (1991**)** 165.
[119] J. Bañuelos, F. López Arbeloa, T. Arbeloa, S. Salleres, J. L. Vilas, F. Amat−Guerri, M. Liras, I. López Arbeloa, J. Fluoresc. 18 (2008) 899.
[120] F. López Arbeloa, J. Bañuelos, V. Martínez, T. Arbeloa, I. López Arbeloa, ChemPhysChem 5 (2004) 1762.
[121] T. V. Gloud, A. Tutar, J−F. Biellmann, Tetrahedron 62 (2006**)** 5084.
[122] V. P. Yakubovskyi, M. P. Shandura, Y. P. Kovtun, Eur. J. Org. Chem. 19 (2009) 3237.
[123] V. P. Yakubovskyi, M. P. Shandura, Y. P. Kovtun, Dyes Pigments 87 (2010**)** 17.
[124] Z. R. Grabowski, K. Rotkiewicz, W. Rettig, Chem. Rev. 103 (2003) 3899.
[125] M. J. Ortiz, I. García−Moreno, A. R. Agarrabeitia, G. Duran−Sampedro, A. Costela, R. Sastre, F. López Arbeloa, J. Bañuelos, I. López Arbeloa, Phys. Chem. Chem. Phys. 10 (2010) 7804.
[126] P. O. Andersson, S. M. Bachilo, R−L. Chen, T. Gillbro, J. Phys. Chem. 99 (1995) 16199.
[127] C. E. Carvalho, I. M. Brinn, A. V. Pinto, M. C. Pinto, J. Photochem. Photobiol. A 136 (2000) 25.
[128] S. Badré, V. Monnier, R. Méallet−Renault, C. Dumas-Verdes, E. Y. Schmidt, A. I. Mikhaleva, G. Levi, A. Ibanez, B. A. Trofimov, R. B. Pansu, J. Photochem. Photobiol. A, 18 (2006) 238.
[129] M. Alvarez, A. Costela, I. García−Moreno, F. Amat−Guerri, M. Liras, R. Sastre, F. López Arbeloa, J. Bañuelos and I. López Arbeloa, Photochem. Photobiol. Sci., 7 (2008) 802.
[130] T. Rohand, W. Qin, N. Boens, W. Dehaen, Eur. J. Org. Chem. (2006) 4658.
[131] A. Cui, X. Peng, J. Fan, X. Chen, Y. Wu, B. Guo, J. Photochem. Photobiol. A 186 (2007) 85.
[132] L. G. S. Brooker, J. Am. Chem. Soc. 87 (1965) 937.
[133] L. G. S. Brooker, A. C. Craig, D. W. Heseltine, P. W. Jenkins, L. L. Lincoln, J. Am. Chem. Soc. 87 (1965) 2443.
[134] D. E. J. G. J. Dolmans, D. Fukumura, R. K. Jain, Nat. Rev. Cancer 3 (2003) 380.
[135] B. Brown, E. A. Brown and I. Walker, Lancet Oncol. 5 (2004) 497.
[136] B. W. Henderson, S. O. Gollnick, CRC Hanboock of Organic Photochemistry and Photobiology, CRC Press, New York, (2004), chap. 145.
[137] G. Jori, CRC Hanboock of Organic Photochemistry and Photobiology, CRC Press, New York, (2004), chap. 146.
[138] T. J. Dougherty, J. G. Levy, CRC Hanboock of Organic Photochemistry and Photobiology, CRC Press, New York, (2004), chap. 147.
[139] K. Berg, Photodynamic Therapy at the Cellular Level, Research Signpost, Kerala, India, (2007), chap. 1.

[140] A. Gorman, J. Killoran, C. O'Shea, T. Kenna, W. M. Gallagher, D. F. O'Shea, J. Am. Chem. Soc., 126 (2004)0 10619.
[141] S. O. MacDonnel, M. J. Hall, A. Byrne, W. M. Gallagher, D. F. O'Shea, J. Am. Chem. Soc., 127 (2005) 16360.
[142] T. Yogo, Y. Urano, Y. Ishitsuka, F. Maniwa, T. Nagano, J. Am. Chem. Soc., 127 (2005) 12162.
[143] S. Erbas, A. Gorgulu, M. Kocakusakogullari and E. U. Akkaya, Chem. Commun. (2009) 4956.
[144] S. Ozlem, E. U. Akkaya, J. Am. Chem. Soc. 131 (2009) 48.
[145] S. H. Lim, C. Thivierge, P. Nowak−Sliwinska, J. Han, H. van den Bergh, G. Wagnières, K. Burgess, H. B. Lee, J. Med. Chem. 53 (2010) 2865.
[146] N. Adarsh, R. R. Avirah, D. Ramaiah, Org. Lett. 12 (2010) 5720.
[147] M. J. Ortiz, A. R. Agarrabeitia, G. Duran−Sampedro, J. Bañuelos, T. Arbeloa, W. A. Massad, H. A. Montejano, N. A. Garcia, I. López Arbeloa, Tetrahedron 68 (2012) 1153.
[148] F. Li, S. I. Yang, Y. Ciringh, J. Seth, C. H. Martin III, D. L. Singh, D. Kim, R. R. Birge, D. F. Bocian, D. Holten, J. S. Lindsey, J. Am. Chem. Soc. 120 (1998) 10001.
[149] H. L. Kee, C. Kirmaier, L. Yu, P. Thamyongkit, W. J. Youngblood, M. E. Calder, L. Ramos, B. C. Noll, D. F. Bocian, W. R. Scheidt, R. R. Birge, J. S. Lindsey, D. Holten, J. Phys. Chem. B 109 (2005) 20433.
[150] M. A. H. Alamiry, A. C. Benniston, G. Copley, K. J. Elliot, A. Harriman, B. Stewart, Y−G. Zhi, Chem. Mater. 20 (2008) 4024.
[151] J. Chen, A. Burghart, A. Derecskei−Kovacs, K. Burgess, J. Org. Chem. 65 (2000) 2900.
[152] T. T. Vu, S. Badré, C. Dumas−Verdes, J−J. Vachon, C. Julien, P. Audebert, E. Y. Senotrusova, E. Y. Schmidt, B. A. Trofimov, R. B. Pansu, G. Clavier, R. Méallet−Renault, J. Phys. Chem. C 113 (2009) 11844.

***